UNCLASSIFIED

SECURITY CLASSIFICATION OF THIS PAGE *(When Data Entered)*

REPORT DOCUMENTATION PAGE		READ INSTRUCTIONS BEFORE COMPLETING FORM
1 REPORT NUMBER NAVENVPREDRSCHFAC Technical Paper No. 6-76	2. GOVT ACCESSION NO.	3. RECIPIENT'S CATALOG NUMBER
4. TITLE *(and Subtitle)* Clearing Fog by Seeding with Charged Water Drops: A Numerical Study		5. TYPE OF REPORT & PERIOD COVERED
		6. PERFORMING ORG. REPORT NUMBER
7. AUTHOR(s) Paul M. Tag		8. CONTRACT OR GRANT NUMBER(s)
9 PERFORMING ORGANIZATION NAME AND ADDRESS Naval Environmental Prediction Research Facility Monterey, CA 93940		10 PROGRAM ELEMENT, PROJECT, TASK AREA & WORK UNIT NUMBERS Air Task 370370G/076B/ 6F52551700 TA:WF52-551-715 NEPRF WU: 055:2-7
11. CONTROLLING OFFICE NAME AND ADDRESS Naval Air Systems Command Department of the Navy Washington, D.C. 20361		12 REPORT DATE May 1976
		13. NUMBER OF PAGES 49
14. MONITORING AGENCY NAME & ADDRESS *(if different from Controlling Office)* Naval Air Systems Command Department of the Navy Washington, D.C. 20361		15. SECURITY CLASS. *(of this report)* UNCLASSIFIED
		15a. DECLASSIFICATION/DOWNGRADING SCHEDULE

16. DISTRIBUTION STATEMENT *(of this Report)*

Approved for public release; distribution unlimited.

17. DISTRIBUTION STATEMENT *(of the abstract entered in Block 20, if different from Report)*

18. SUPPLEMENTARY NOTES

19. KEY WORDS *(Continue on reverse side if necessary and identify by block number)*

Coalescence
Collision-coalescence
Fog
Fog Dispersal
Warm Fog

20. ABSTRACT *(Continue on reverse side if necessary and identify by block number)*

A numerical study of the use of highly charged water drops to clear warm fog has been conducted. The polarization of neutral fog droplets and their capture by the charged drops is the mechanism studied. A multi-leveled microphysical model is used to investigate the degree of visibility improvement resulting from variations in seeding drop size and charge,

DD FORM 1 JAN 73 1473 EDITION OF 1 NOV 65 IS OBSOLETE
S/N 0102-014-6601

UNCLASSIFIED

SECURITY CLASSIFICATION OF THIS PAGE *(When Data Entered)*

20. Abstract (continued)

the type of fog being seeded, and the concentration of seeding material. An evaluation of this technique is made by comparing model results to comparable numerical experiments of hygroscopic seeding, a technique that has been field tested on several occasions.

CONTENTS

ACKNOWLEDGMENTS

I wish to thank those members of the Naval Weapons Center, particularly Mr. John Carroz, who provided important data concerning the operational aspects of this study. I am equally indebted to Ms. Winona Carlisle who typed the manuscript and Mr. Richard Clark who provided the excellent figures and illustrations.

AN (1) AD-A027 410
FG (2) 040200
CI (3) (U)
CA (5) NAVAL ENVIRONMENTAL PREDICTION RESEARCH FACILITY MONTEREY CALIF
TI (6) Clearing Fog by Seeding with Charged Water Drops: A Numerical Study.
TC (8) (U)
AU (10) Tag,Paul M.
RD (11) May 1976
PG (12) 52p
RS (14) NEPRF-Technical Paper-6-76
PJ (16) A370-370G/076-b/6f52-551-700
PJ (16) WF52-551
TN (17) WF52-551-715
RC (20) Unclassified report
DE (23) *Fog dispersal, *Visibility, Seeding, Water, Drops, Concentration(Composition), Rates, Sizes(Dimensions), Mathematical models, Coalescence, Polarization
DC (24) (U)
ID (25) Warm fog, Hygroscopic seeding
IC (26) (U)
AB (27) A numerical study of the use of highly charged water drops to clear warm fog has been conducted. The polarization of neutral fog droplets and their capture by the charged drops is the mechanism studied. A multi-leveled microphysical model is used to investigate the degree of visibility improvement resulting from variations in seeding drop size and charge, the type of fog being seeded, and the concentration of seeding material. An evaluation of this technique is made by comparing model results to comparable numerical experiments of hygroscopic seeding, a technique that has been field tested on several occasions. (Author)
AC (28) (U)
DL (33) 01
CC (35) 407279

Approved for public release;
Distribution unlimited

NAVENVPREDRSCHFAC
Technical Paper No. 6–76

CLEARING FOG BY SEEDING WITH CHARGED WATER DROPS: A NUMERICAL STUDY

by

PAUL M. TAG

MAY 1976

NAVAL ENVIRONMENTAL PREDICTION RESEARCH FACILITY
MONTEREY, CALIFORNIA 93940

1. INTRODUCTION

The use of electrostatic effects between droplets has been postulated as a potential mechanism for dissipating warm fog. Two separate effects, summarized in Figure 1, must be considered with respect to electrically enhanced coalescence. One is the result of an applied electric field which polarizes all droplets. Tag (1976) considered this possibility and found that extreme electric fields are necessary to produce a worthwhile improvement in visibility, and then only in fogs with relatively large water droplets. The second effect is the focus of study in this paper.

The effect of electric fields and charges on collision-coalescence has long been recognized. Lord Rayleigh (1879) noted the effect of electricity on drops emitted from a water jet. In 1923, an article in Scientific American commented on a proposal that charged sand particles be used to clear a fog. Pauthenier (1950) suggested that charged water drops be used. Carroz et al. (1972) made an initial attempt at determining visibility improvement as the result of charged seedings, but considered only monodisperse fog and treatment drops in conjunction with a continuous growth process for the charged drops. Tag (1976) provides a more complete history of both electrostatic effects.

Using a microphysical fog model, this study will examine charged drop seeding as a fog dispersal technique. The purpose is to evaluate the potential of this method, as well as to isolate those parameters which would most control the degree of visibility improvement in an experimental environment.

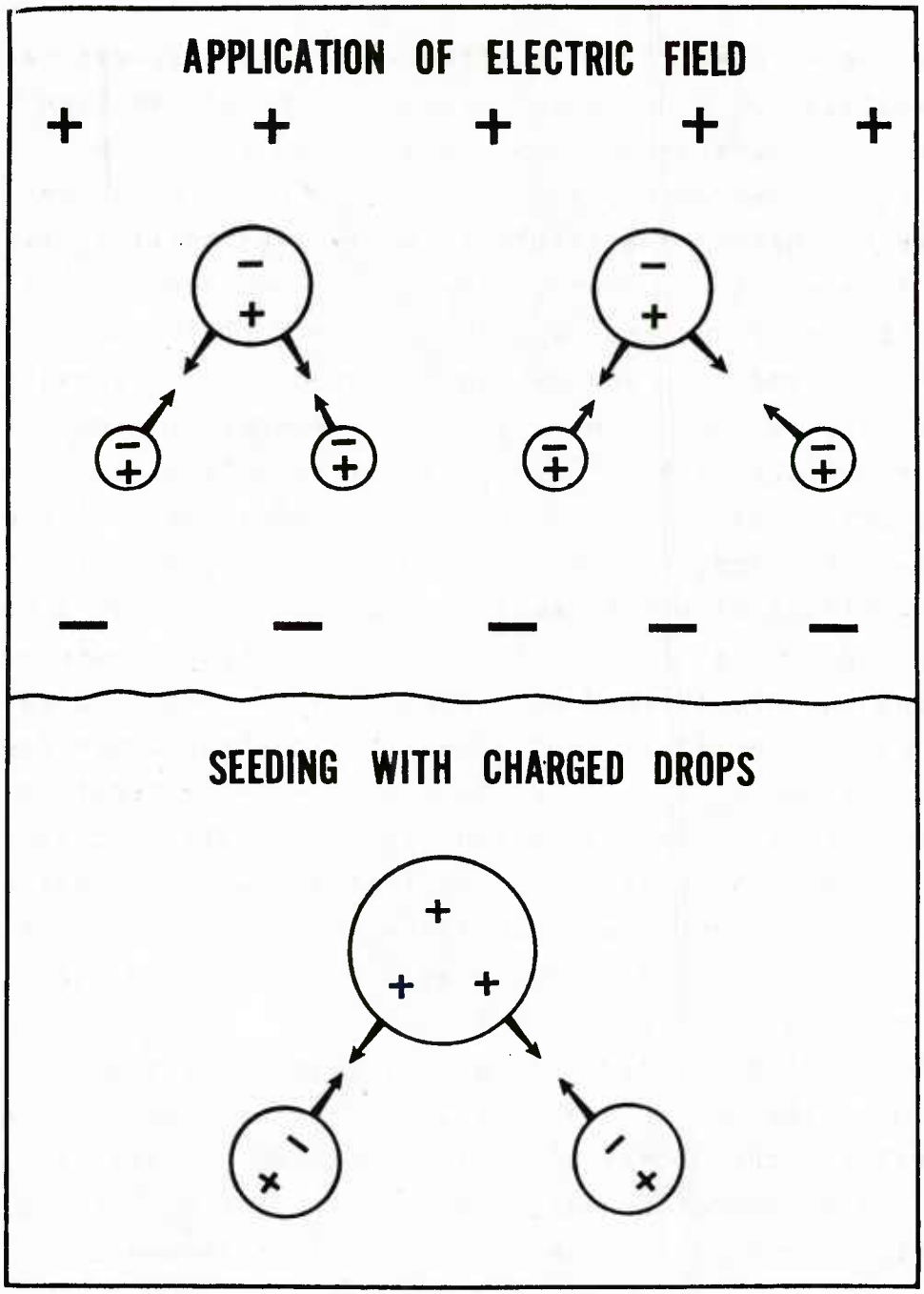

Figure 1. The two separate aspects of electrically enhanced coalescence.

2. PRELIMINARY CONSIDERATIONS

Before proceeding, a discussion of drop charge and associated collision efficiencies is warranted. In the situation simulated previously (Tag, 1976), a uniform electric field was applied continuously to the entire fog, resulting in collision efficiencies which remained unchanged for any drop size-pair combination. The numerical simulation becomes more complicated when individual drop charges must be conserved with every collision and also result in collision efficiencies that change for every size combination with every time step. Difficulties arise in finding an efficient method of determining appropriate collision efficiencies.

a. Drop Charging

It is necessary to understand the charging limitations appropriate for water drops. Lord Rayleigh (1882) was the first to derive the limit to which a water drop can be charged before rupturing:

$$Q = \sqrt{16\ \pi\ \sigma\ r^3} \quad \text{esu} \qquad (1)$$

where σ is the surface tension and r the radius of the drop. Equation (1) is commonly referred to as the "Rayleigh Limit" and defines that charge at which electrical forces which tend to rupture the drop exactly balance the surface tension holding the drop together. Empirical verification of this limit has been attempted by several workers. Using charged oil drops with radii 0.1 to 10 microns, Hendricks (1962) found very close agreement to the Rayleigh theoretical curve. More recent verification was made by Schweizer and Hanson (1971). Using drops made of n-octanol with a size range 7.5 to 20 microns, the measured charge to mass ratios of the drops at breakup were within a standard deviation of 4% of the Rayleigh Limit.

A second point that must be considered is the length of time a drop can hold its charge. If a discharge should be instantaneous, no advantage would be gained from an initially large charge. Vonnegut (Moore, 1973), however, states that objects supported in the atmosphere will lose charge at a rate corresponding to a half-life of 10 to 20 minutes. Schweizer and Hanson, in the experiments described above, found that their drops, which were often charged completely to the Rayleigh Limit, occasionally lost some charge, but that this loss was never very large. In this paper, it is assumed that such leakage would likewise be small in an airflow, as found in the wake of an aircraft. Because the actual charges that are simulated are only a fraction of the Rayleigh Limit maximum (see below), and also because of the rapidity with which these drops should grow, the assumption of negligible charge loss is probably acceptable.

Finally, assuming that a large charge is desirable and will remain on the drop, what are the operational limitations in achieving that charge? Carroz and Keller (1976) conducted laboratory experiments to isolate parameters important for achieving maximum drop charge. Using induction charging, they found that the degree of charging is a function of nozzle type, liquid flow rate, airflow speed past the nozzle, voltage, and several other factors. In general, they found that, using cone-type nozzles, drops could be charged to a maximum of 25% of the Rayleigh Limit, with an average value closer to 15%. These figures provide realistic limitations to the drop charges that are used in the numerical experiments conducted in this study.

b. Collision Efficiencies

In order to ascertain the effect of charged drops in a microphysical model, one must have precise values of collision efficiency for the drop interactions. As outlined

in Tag (1976), various theoretical and experimental studies have defined efficiencies for various alignments of electric fields and drop charge combinations. Because of non-linearity of the results, however, analytic solutions and numerical approximations have been few. Using a trajectory model based on work by Davis (1964), and Davis and Sartor (1967), Paluch (1970) compared computed efficiencies to analytically derived values for certain simplified cases. Unfortunately, only oppositely charged drops were considered. For the situation here, a charged-neutral interaction is the one of interest.

Although not considered by Paluch, the trajectory model noted above is capable of simulating charged-neutral combinations. Dr. Doyne Sartor of NCAR offered his computer program for computing these efficiencies. It was intended that this model be used in conjunction with the microphysical fog model. It soon became clear, however, that the models could not be used together. On a CDC 6500, one collision efficiency calculation takes on the order of 20 seconds. Since several hundred efficiency calculations would be necessary per time step, it was realized that a simplifying assumption would be necessary.

An earlier paper by Cochet (1952) provided this simplification. Cochet was interested in the possibility of seeding neutral clouds with charged drops with the idea of initiating precipitation. In the process of calculating the growth of a charged drop, he derived an expression for collision efficiencies for charged-neutral combinations. As Paluch did in her work, Cochet made certain approximations in his derivation from the equation of motion, the primary one being that the inertia of the charged collector modifies negligibly the flow field around itself. Such an assumption is quite valid for small, highly-charged collectors, but becomes increasingly suspect as the collector increases in size or as the charge/mass ratio decreases. Cochet found this approximation to be

$$Y_c^2 = \frac{1}{r_i^2}\left[\frac{45}{16}\frac{\lambda\, q^2\, r_n^2}{\rho\, g\,(r_i^2 - r_n^2)}\right]^{\frac{2}{5}} \qquad (2)$$

where Y_c is the linear collision efficiency, $\lambda = (\varepsilon-1)/(\varepsilon+2)$ and ε the dielectric constant, ρ the density of water, q charge (esu), and r_i and r_n are the radii of the collector and collected drops, respectively. Notice that collision efficiency is not a function of the charge sign. In this study, all drop charges will be assumed to be of the same sign, and positive.

Cochet recognized Eq. (2) as an approximation and attempted to determine its inaccuracy. Figure 2, taken directly from Cochet's 1952 paper, shows a comparison between Eq. (2) (dot-dashed lines) and actual values (solid lines) for a collector drop charge of 4×10^{-4} esu (1 coulomb = 3×10^9 esu). This charge corresponds, approximately, to 20 and 2% of the Rayleigh Limit for 10 and 50 microns radius respectively. The term "actual" refers to efficiencies obtained without the approximations inherent in the derivation of Eq. (2). Cochet determined "actual" collision efficiencies by performing trajectory calculations graphically, instead of numerically as done in the NCAR model. To ascertain the accuracy of his graphical technique, several points on Cochet's curves were recalculated using the NCAR model. Remarkably, nearly all calculated values lay within the readable error in Figure 2, due to the care with which Cochet drew his trajectories or, alternately, to the credit of the NCAR model. For a given charge, therefore, Figure 2 shows that the approximation is generally an over-estimator as the collector increases in size or, as noted above, inertia becomes more and more a factor.

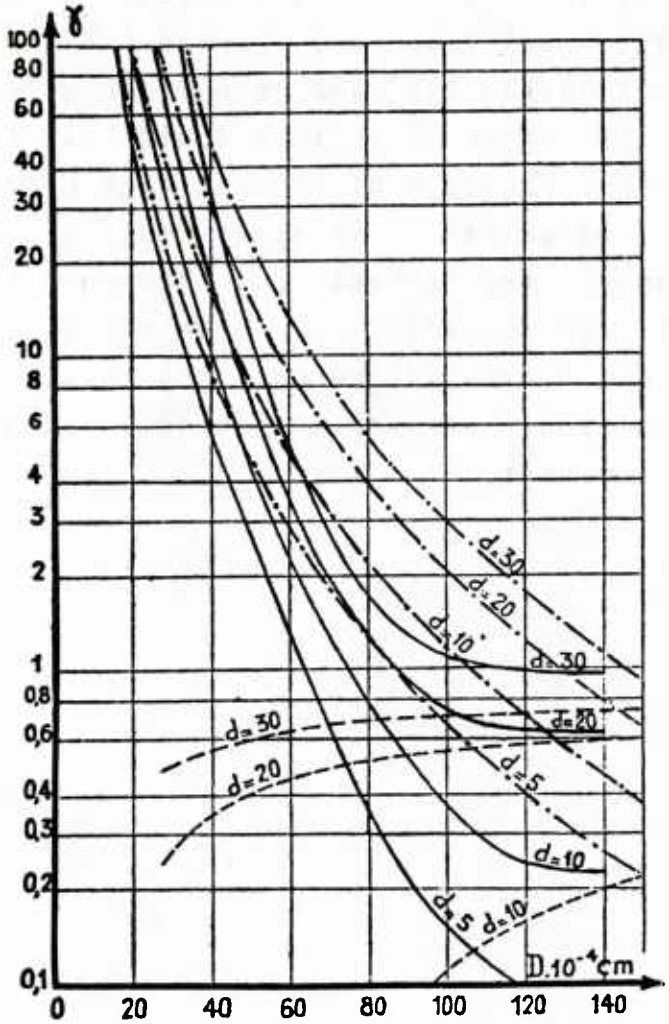

Figure 2. Charged-neutral collision efficiencies (γ -- Cochet's symbol for this variable), actual (solid) and from Eq. 2 (dot-dashed), for collector diameters D and various collected diameters, d, for a collector charge of 4.0E-4 esu (taken from Cochet (1952)). The dashed lines represent hydrodynamic efficiencies (after Langmuir).

Although obviously inaccurate under certain conditions, Cochet's equation is used in this study for the following reasons. Firstly, no better approximation could be found. Secondly, the equation is accurate under those conditions which are being, at least initially, simulated (i.e., highly charged, relatively small droplets). Because Figure 2 was drawn for drops all having the same absolute charge, more error appears at the larger sizes than would have if all drops had a certain percentage of the Rayleigh Limit charge. Additionally, the approximation is always most accurate when collision efficiencies are largest, and thus when they have their most impact. Inaccuracies can be better tolerated when their effect is less. Finally, recognizing that inaccuracies will almost always appear as over-estimates, one has an understanding of the bias.

3. MODEL DESCRIPTION

The basic model is the same as that described in Tag (1976). At each of ten model levels a fog droplet spectrum is specified and evolves as the result of collision-coalescence, sedimentation, and turbulent mixing. Visibility is computed from the drop spectra. The change required in the model for this study is the addition of a second "treatment" spectrum, subject to the same processes as above, but which also interacts with the fog spectra. Because seeding drops will carry a charge and fog droplets are assumed neutral, a separation of the spectra is necessary. In addition, the total charge assigned to the treatment categories must be conserved and followed.

Letting N_F and N_T (as a function of radius r and height z) be the average number density of fog and treatment (charged) drops, respectively, the two spectra evolve according to the following:

$$\frac{\partial N_F}{\partial t} = -w(r)\,\frac{\partial N_F}{\partial z} + K\,\frac{\partial^2 N_F}{\partial z^2} + FF + FT_{\text{Loss F}} \qquad (3)$$

$$\frac{\partial N_T}{\partial t} = -w(r)\,\frac{\partial N_T}{\partial z} + K\,\frac{\partial^2 N_T}{\partial z^2} + TT_{\text{Loss T}} + TT_{\text{Gain T}} + FT_{\text{Loss T}} + FT_{\text{Gain T}} \qquad (4)$$

where collision-coalescence is represented by the following interaction combinations:

FF = Fog - Fog
TT = Treatment - Treatment
FT = Fog - Treatment

Because two separate spectra are represented simultaneously, these three combinations are necessary. However, after a few preliminary computer experiments, it was decided to eliminate FF interactions. Since it had been intended that empirical spectra from mature fogs be used, little advantage was seen in allowing the fog spectrum to evolve further. Consequently, FF interactions were set to zero.

Notice that there are no fog-treatment interactions which result in a "gain" for the fog spectrum. This convention was chosen so as to result always in the dilution of the treatment drop and its subsequent placement back into the treatment spectrum. This segregation is mandatory since the electrostatic efficiencies provided by Eq. (2) are valid only for charged-neutral combinations. For this reason, the resulting drop of a collision involving a treatment drop is always regarded as a treatment drop. Alteration of the charge/mass ratio of treatment drops, as a result of collisions with neutral and other charged drops, is essential in determining appropriate collision efficiencies. In addition, besides forcing segregation of the two spectra, this convention permits movement of water from one spectrum to the other (a measure of the rapidity with which treatment is working) to be followed quite easily.

The above terms involving collision-coalescence can be summarized by the following:

$$-N_T(i)\sum_{n=1}^{i-1} P_T(i,n)B(i,n) - \sum_{n=i+1}^{M} N_T(n)P_T(n,i) = TT(i)_{Loss\ T}\Delta t \tag{5}$$

$$N_T(i-1)\sum_{n=1}^{i-2} P_T(i-1,n)B(i-1,n) = TT(i)_{Gain\ T}\Delta t \tag{6}$$

$$-N_A(i) \sum_{n=1}^{i-1} P_B(i,n)B(i,n) - \sum_{n=i+1}^{M} N_B(n)P_A(n,i) = \begin{cases} FT(i)_{\text{Loss } F}\Delta t \\ \text{when } A=F, B=T \\ FT(i)_{\text{Loss } T}\Delta t \\ \text{when } A=T, B=F \end{cases} \tag{7}$$

$$N_F(i-1) \sum_{n=1}^{i-2} P_T(i-1,n)B(i-1,n) + N_T(i-1) \sum_{n=1}^{i-2} P_F(i-1,n)B(i-1,n)$$

$$= FT(i)_{\text{Gain } T}\Delta t \tag{8}$$

As in the first part of this study, B is the drop partitioning factor, i and n refer to category numbers and M is the total number of categories. P(i,n) is defined as the probability that an ith will collect an nth category drop in time Δt:

$$P(i,n) = V(i,n)\, N(r_n)\, \Delta t \tag{9}$$

where V(i,n), as defined by Berry (1967), is the collection kernel:

$$V(i,n) = \pi r_i^2 \left[Y_c(r_i, r_n, q_i)\right]^2 E\left[w(r_i) - w(r_n)\right] \tag{10}$$

Y_c is the linear collision efficiency as used by Shafrir and Neiburger (1963) and E is the coalescence (as opposed to collision) efficiency. For reasons similar to those outlined in Tag (1976), the coalescence efficiency will be assumed to be unity. The mathematical approximations of Wobus et al. (1971) are used for the drop terminal velocities, w(r).

Assuming that each treatment drop is initially assigned an electrostatic charge, the movement of this charge as the result of collision-coalescence and vertical transfer must be followed. Several methods of charge allocation and conservation were considered. It was decided that a continuing assignment of a single charge per drop-category would be adequate, rather than maintaining an array of charges per category as collection proceeds. The justification for this decision stems from Eq. (2). An analysis of Cochet's equation shows that variation of collector drop radius is much more important than variation of charge. A doubling of radius results in an order of magnitude change in collision efficiency; a similar doubling of charge results only in a doubling of efficiency. For this reason, assignment of an average charge per drop category is a reasonable assumption. Consequently, for collection, the procedure involves only simple averaging of charge for those drops entering, as well as those remaining in, a given size-category:

$$q_T(i)_{NEW} =$$

$$\frac{q_T(i)_{OLD}\ (N_T(i) + \Delta N_T(i)) + q_{TT}(i)TT(i)_{GAIN\ T} + q_{FT}(i)FT(i)_{GAIN\ T}}{N_T(i) + \Delta N_T(i) + TT(i)_{GAIN\ T} + FT(i)_{GAIN\ T}}$$

where, (11)

$$\Delta N_T(i) = TT(i)_{LOSS\ T} + FT(i)_{LOSS\ T} \quad \text{and,}$$

$$q_{TT}(i) = N_T(i\text{-}1) \sum_{n=1}^{i-2} P_T(i\text{-}1,n)B(i\text{-}1,n) \left[q_T(i\text{-}1) + q_T(n)\right] \Big/ TT(i)_{GAIN\ T}\ \Delta t \quad (12)$$

and,

$$q_{FT}(i) = N_F(i-1) \sum_{n=1}^{i-2} P_T(i-1,n)B(i-1,n)\, q_T(n) + N_T(i-1) \sum_{n=1}^{i-2} P_F(i-1,n)B(i-1,n)\, q_T(i-1) \Big/ FT(i)_{GAIN\ T} \Delta t, \quad (13)$$

recalling that $q_F(i-1)$ and $q_F(n)$, by definition, are zero. A similar procedure is used for conservation of charge as the result of movement between model levels. Although Eqs. (11)-(13) conserve total drop charge, they more importantly permit the charge-to-mass ratio to change as the result of collection. It is this ratio which determines the rate of collection of fog droplets.

In assigning appropriate collision efficiencies for the several collection combinations, it will be assumed that only treatment-collecting-fog interactions have collision efficiencies other than the normal hydrodynamic ones. Cochet's equation is valid only for charged-neutral collections. Obviously, the assumption that hydrodynamic efficiencies apply for charged collecting charged, and neutral collecting charged, droplets is incorrect. Because no simple approximation is available for these cases, hydrodynamic efficiencies are arbitrarily used. Two considerations, however, minimize the effect of this assumption. First, although all treatment drops of different size have a different charge (a percentage of the Rayleigh Limit), it is assumed that all charges are of the same sign. Consequently, collisions should not be enhanced for charged-charged interactions. Second, there will be few FT collisions in which the collector is a fog drop since the charged drops must generally be larger than the fog droplets for the simulated mechanism to be effective.

4. AN ANALYSIS OF THE COLLECTION KERNEL

Prior to conducting the numerical simulations, a look at the collection kernels (V) for charged and uncharged collectors is warranted. The kernel provides a much better idea of sweepout effect than the collision efficiency alone since the fall velocity difference is included in V. Figure 3 gives a comparison between the neutral (Figure 3a) and two charged collector cases. The numerical fits by Berry (1967) of the Shafrir-Neiburger collision efficiencies are used for the neutral collectors, and Cochet's equation provides electrostatic efficiencies for the 15 and 30% Rayleigh Limit cases. These percentages provide reasonable outlines to the experimental limits cited earlier. Note that the absolute collector charge changes with radius since the Rayleigh Limit increases with radius.

A quick comparison of the three cases reveals the strong effect of charge on the sweepout rate. Increases from one to two orders of magnitude are evident. A closer examination shows, however, that such increases are sharply curtailed as the collector size increases beyond 25 microns! As a result, one would conclude that seeding drops should be relatively small in size. This conclusion is enhanced when one considers that the volume of liquid required increases as the radius cubed.

A comparison of Figures 3b or c to 3a shows that, in addition to increasing in absolute magnitude, the curve for any size collector is shifted to the right -- implying better collection of nearly equal-sized drops. This shift results from the rapid increase of collision efficiency as the collected drop size approaches the collector radius.

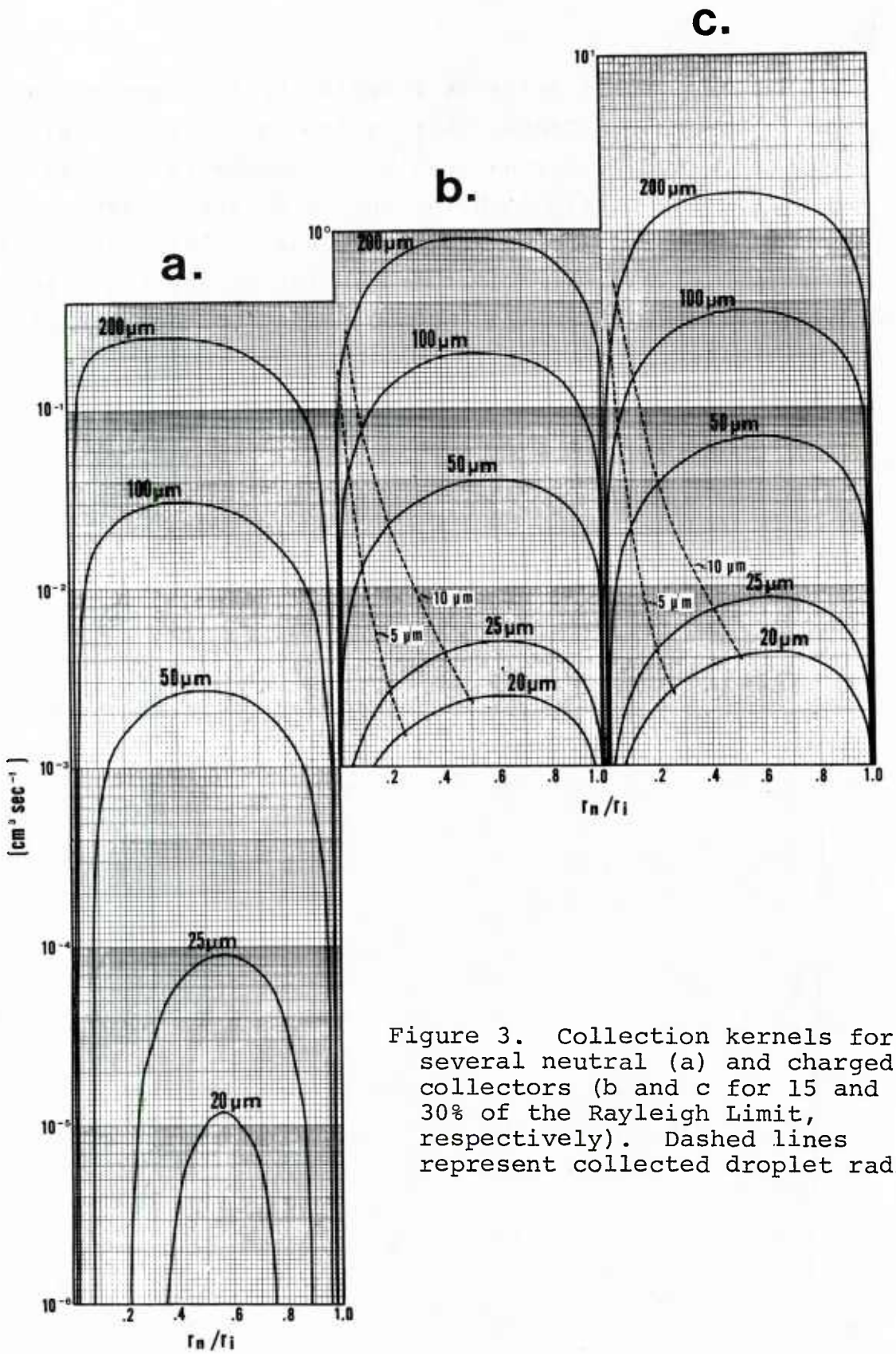

Figure 3. Collection kernels for several neutral (a) and charged collectors (b and c for 15 and 30% of the Rayleigh Limit, respectively). Dashed lines represent collected droplet radii.

One additional point is revealed by the dashed lines in Figures 3b and c. These lines follow two sizes of collected droplets, 5 and 10 microns radius -- two sizes typical of fog droplet spectra. Both for 3b and c, the larger fog radius has the better chance of being collected. This observation again implies, as was also the case for an applied electric field, that results will be closely tied to the type of fog being treated.

5. MODEL INPUT

The two fog types used in Tag (1976) are reused here and are shown in Figure 4. The measurements responsible for Fog A were taken in the Panama Canal Zone and are typical of fogs forming near a maritime influence. This spectrum has a mean volume radius of 10.8 microns, a liquid water content (LWC) of 0.39 gm m^{-3}, and produces a calculated visibility of 143 m. Fog B is based on data taken in the valley fogs of California in which LWC's are typically below 0.1 gm m^{-3}, maximum drop radii are approximately 7-8 microns, and mean sizes average around 3 microns (Reinking, 1975). Fog B results in a calculated mean radius of 2.9 microns and a visibility of 77 m. Spectra from actual data from valley fogs yielded spectral shapes very similar to that of Fog A; consequently, the same spectral shape is used for both fogs. These two cases outline realistic limits of several important fog parameters and should allow assessment of these limits with regard to seeding. As in Tag (1976), a constant exchange coefficient of 2 m^2 sec^{-1} is again used.

Probably the most important input data are the seeding spectrum and its associated charge. Carroz and Keller (1975), after assessing the advantages of various nozzle types for an operational seeding program, chose 30° cone angle nozzles with 4.2 gallon per hour (GPH) flow rates (at 300 psi). Limited data were available for this nozzle. However, a size distribution was available for a 1.0 GPH nozzle and the spray patterns are considered similar for the two. The tabular portion of Figure 5 represents empirical data for this nozzle (Tate and Olson, 1962); the accompanying plot shows the mass distribution for a 1 gm m^{-3} total water mass. A charge is assigned to each size category in the model appropriate to this seeding distribution. Using 15% of the Rayleigh Limit

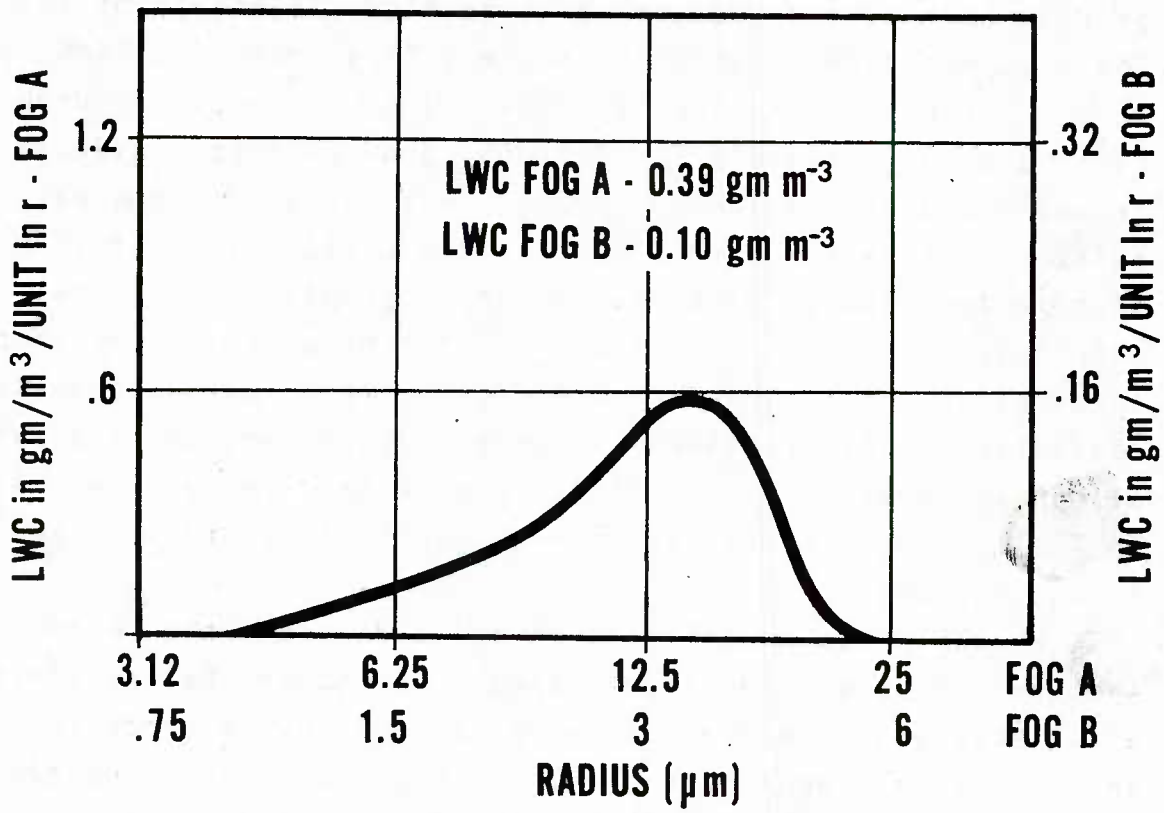

Figure 4. Water mass distribution for Fogs A and B.

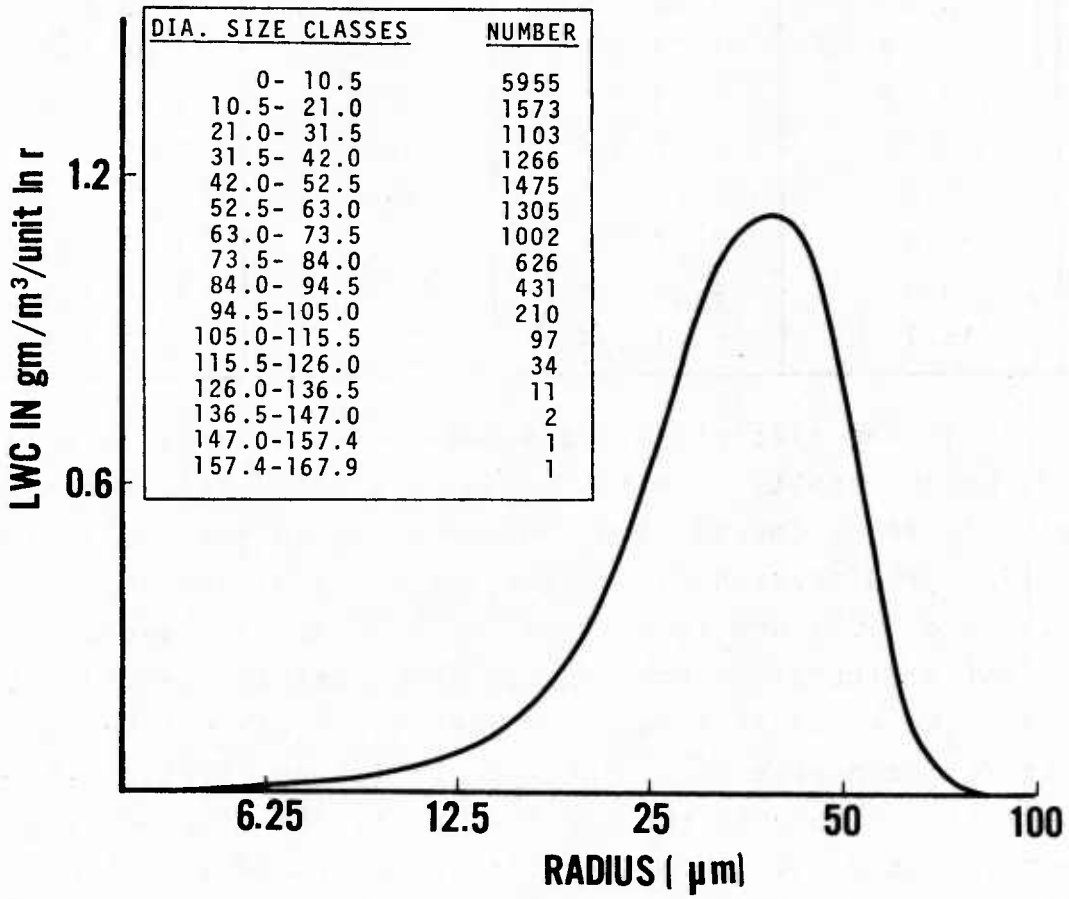

Figure 5. Water mass distribution for treatment spray spectrum. Tabular inset is empirical data from which the spectrum was fashioned (after Tate and Olson (1962)).

as an average charge, Table 1 lists this charge for each of the model's size categories applicable to the distribution shown in Figure 5.

Table 1

Radius (μm)	Charge (esu)	Radius (μm)	Charge (esu)
4.44	8.49 E-5	19.7	7.93 E-4
5.23	1.08 E-4	23.2	1.01 E-3
6.18	1.39 E-4	27.4	1.30 E-3
7.29	1.79 E-4	32.3	1.67 E-3
8.60	2.29 E-4	38.1	2.13 E-3
10.1	2.91 E-4	45.0	2.74 E-3
12.0	3.77 E-4	53.1	3.51 E-3
14.1	4.80 E-4	62.7	4.50 E-3
16.7	6.19 E-4	73.9	5.76 E-3

As in the electric field simulations, a Δz of 15 m is used, which results in a fog of 150 m depth. This depth is realistic for a coastal fog and not uncommon for valley fogs. The 15 m grid spacing was chosen for two additional reasons. First, the 150 m provides a realistic height above ground from which aircraft operations could be safely carried out. Second, the aircraft from which seeding operations have, in practice, been planned is the B-26 (Reinking, 1975). An empirical estimate of the vertical diffusion of a seeding plume injected into this aircraft's wake is 25-30 m (see below). Insertion at two model levels provides a reasonable simulation of the vertical depth through which material would be distributed.

It is necessary to consider both the type of aircraft and its speed in determining the concentration of water that is to be distributed into the aircraft wake. Smith and MacCready (1963) state that the flow field of an aircraft wake is contained in an oval area $A = 1.69\ b^2$, where b is

the aircraft wingspan. Assuming an even distribution within this wake, Figure 6 relates seeding concentrations to seeding rates for several speeds of the B-26 aircraft (b = 21.79 m). While there are sure to be wide variations of concentration within the plume, the use of this diagram does provide a first order estimate of liquid concentration. Reinking (1975), in describing an airborne spray system for charged drops, stated that the system was capable of spraying at a rate of 55 gal min^{-1}. Depending on the speed of the aircraft, Figure 6 suggests that this rate results in concentrations ranging from 0.05 to 0.10 gm m^{-3}; such estimates will provide a basis for model seeding concentrations.

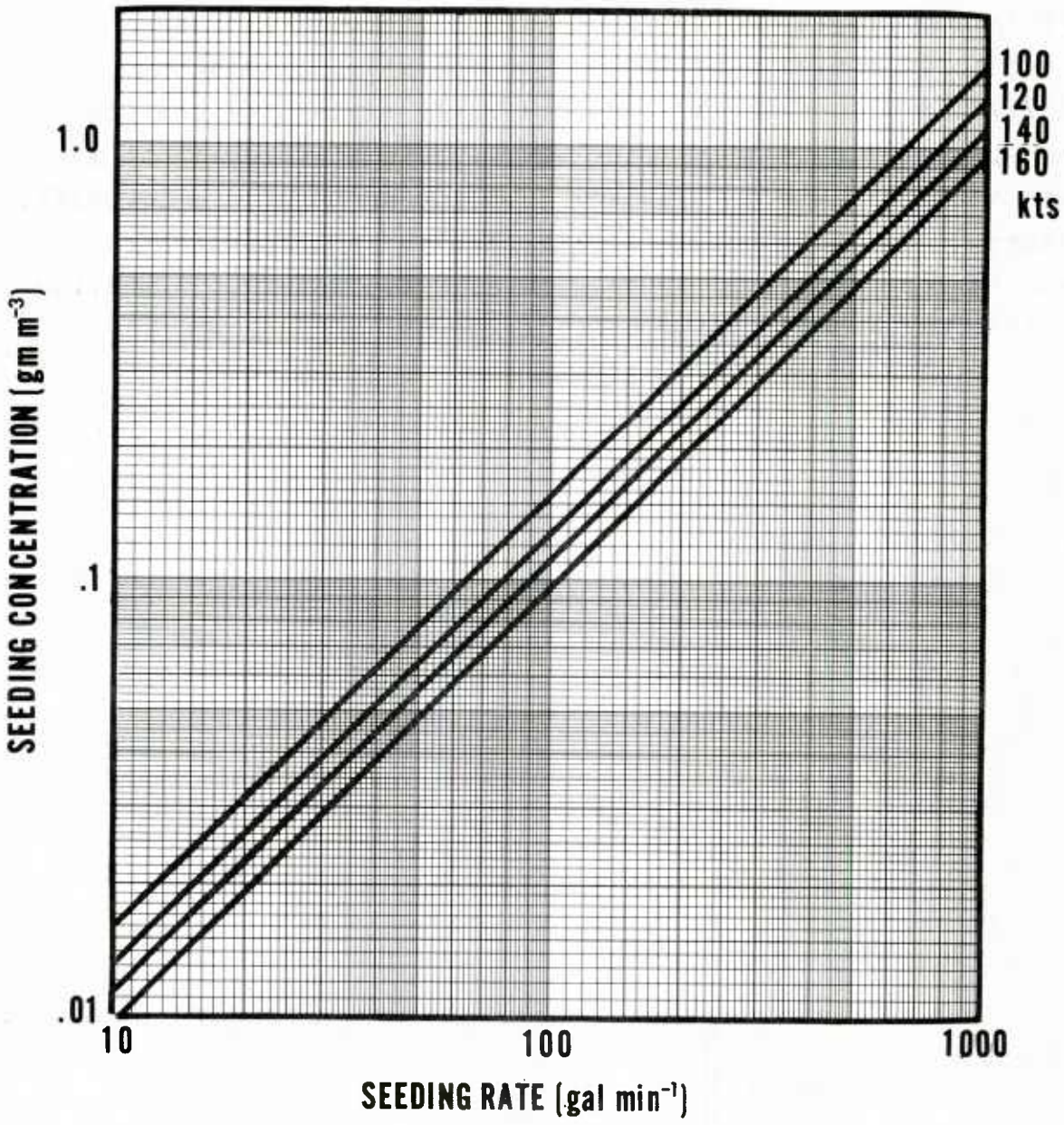

Figure 6. Seeding concentrations resulting from various seeding rates of the B-26 aircraft.

6. NUMERICAL RESULTS

a. Experiment Set I - Variation of Fog Type

Using the fog and seeding spectra described in section 5, six numerical experiments were completed. Two of these were designated as controls and represented water seedings with no associated charge. All experiments were run for 15 minutes fog time with a time step of 2.5 sec. It was felt that this period of time provided a reasonable goal for operational usefulness. In addition, fog regeneration and mixing into the seeded area (effects for which the model has no capability) would greatly mask results beyond this time period.

Using the nomogram shown in Figure 6, a 55 gal min^{-1} seeding rate can produce a maximum treatment concentration of approximately 0.1 gm m^{-3}. The numerical seedings of Fogs A and B were made using this concentration and the spectrum described in Figure 5. Assuming an aerial release at the top of the fog, material is inserted at levels 9 and 10 -- corresponding to the depth suggested previously. To assess the potential of a larger seeding rate, the remaining two cases were run with 0.2 gm m^{-3} concentrations.

Figure 7 gives visibility improvement as a function of height for the above seeding variations in Fog A (initial visibility = 143 m). Figure 7a represents seeding with electrically-neutral water drops, using the larger seeding concentration of 0.2 gm m^{-3}. Although a small change does occur, most of the improvement at fog top is only the result of preferential fallout of the larger fog particles. The neutral seeding drops are relatively inefficient collectors. Figure 7b represents seeding drops charged to 15% of the Rayleigh Limit, as given in Table 1. Figure 7c represents the same seeding spectrum but with twice the seeding amount.

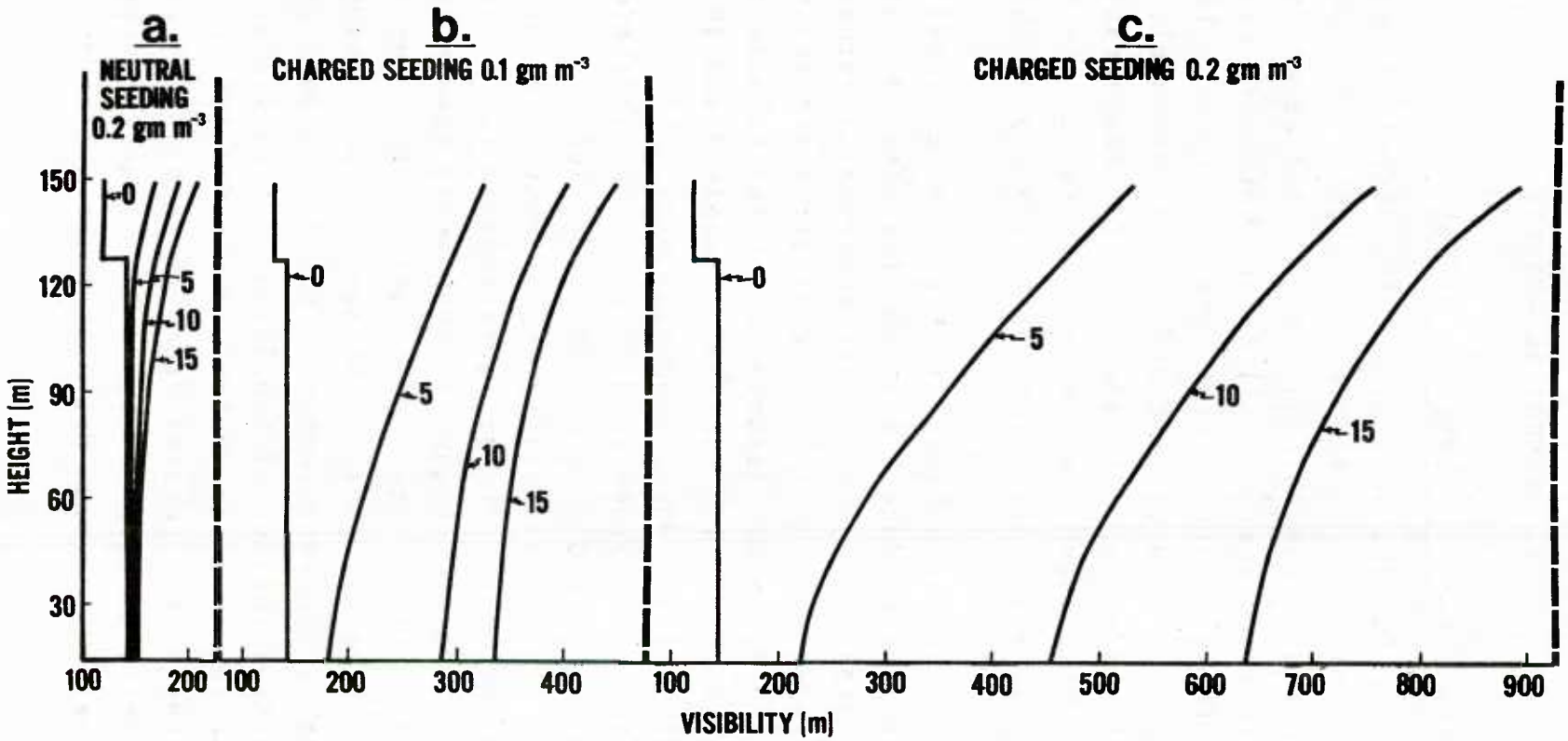

Figure 7. Visibility as a function of time (min) and height for three seeding variations in Fog A.

The effect of charge on visibility improvement is evident. Maximum impact on visibility occurs at the top of the fog where the charge/mass ratio of the seeding drops is largest. As collection of neutral fog droplets proceeds, the charge/mass ratio of these collectors decreases. Counteracting this effect, however, is the fact that the collectors are increasing in absolute size. Consequently, the effect of charge density decrease is offset somewhat as the seeding drops fall through the fog.

As shown in Figure 7c, a larger seeding concentration results (at least for this case) in more visibility improvement. The transfer of water from the fog to the seeding spectrum for this experiment is demonstrated in Figure 8. At alternate levels of the model, LWC for fog and treatment is plotted as a function of time. Seeding material has an initial maximum at 135 and 150 m (level 10 not shown). As water moves from one spectrum to the other as the result of collection, this maximum moves downward at a speed corresponding to the fall velocity of the average drop sizes. More than 80% of the fog LWC is removed at all levels. A look at the spectra, however, indicates that water is preferentially removed at the larger sizes. Whereas over 90% of 20 μm droplets are removed at 15 m, only 45% of 3 μm fog particles are swept out. This result is consistent with the collection kernel in Figure 3b. This bias, unfortunately, favors the wrong end of the spectrum. An LWC of 0.1 gm m^{-3} which at 20 μm radius will reduce visibility to less than 1000 m, will restrict visibility at 3 μm to approximately 50 m (Johnson, 1972). For this reason, the 80% LWC reduction is not as impressive as it might be.

Figure 9 represents indentical seedings of Fog B, the narrow spectral, small droplet fog typical of inland California. The calculated initial visibility is 77 m.

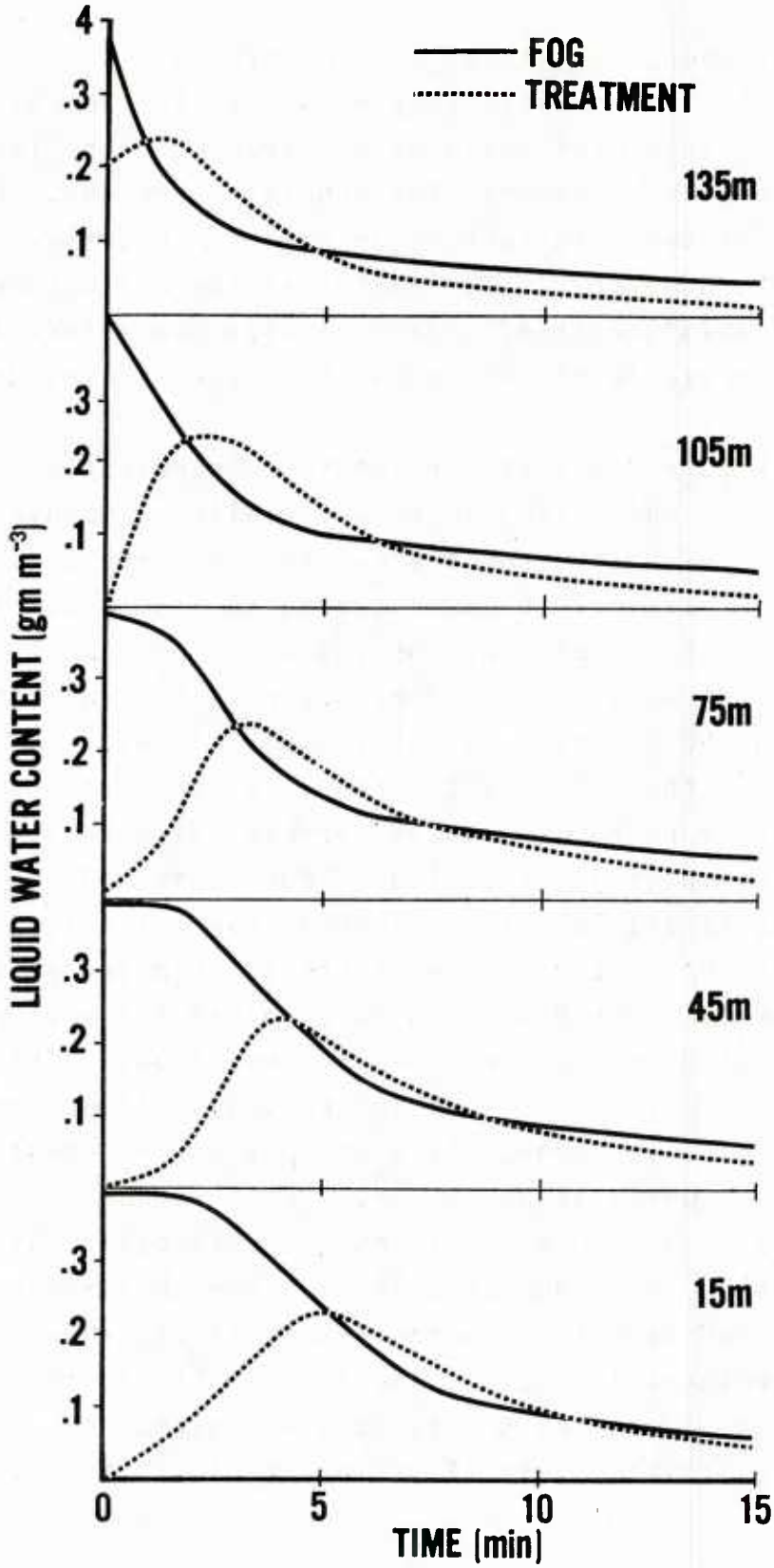

Figure 8. For alternate model levels, the change in fog and treatment LWC for experiment depicted in Figure 7c (Fog A with charged seeding of 0.2 gm m^{-3}).

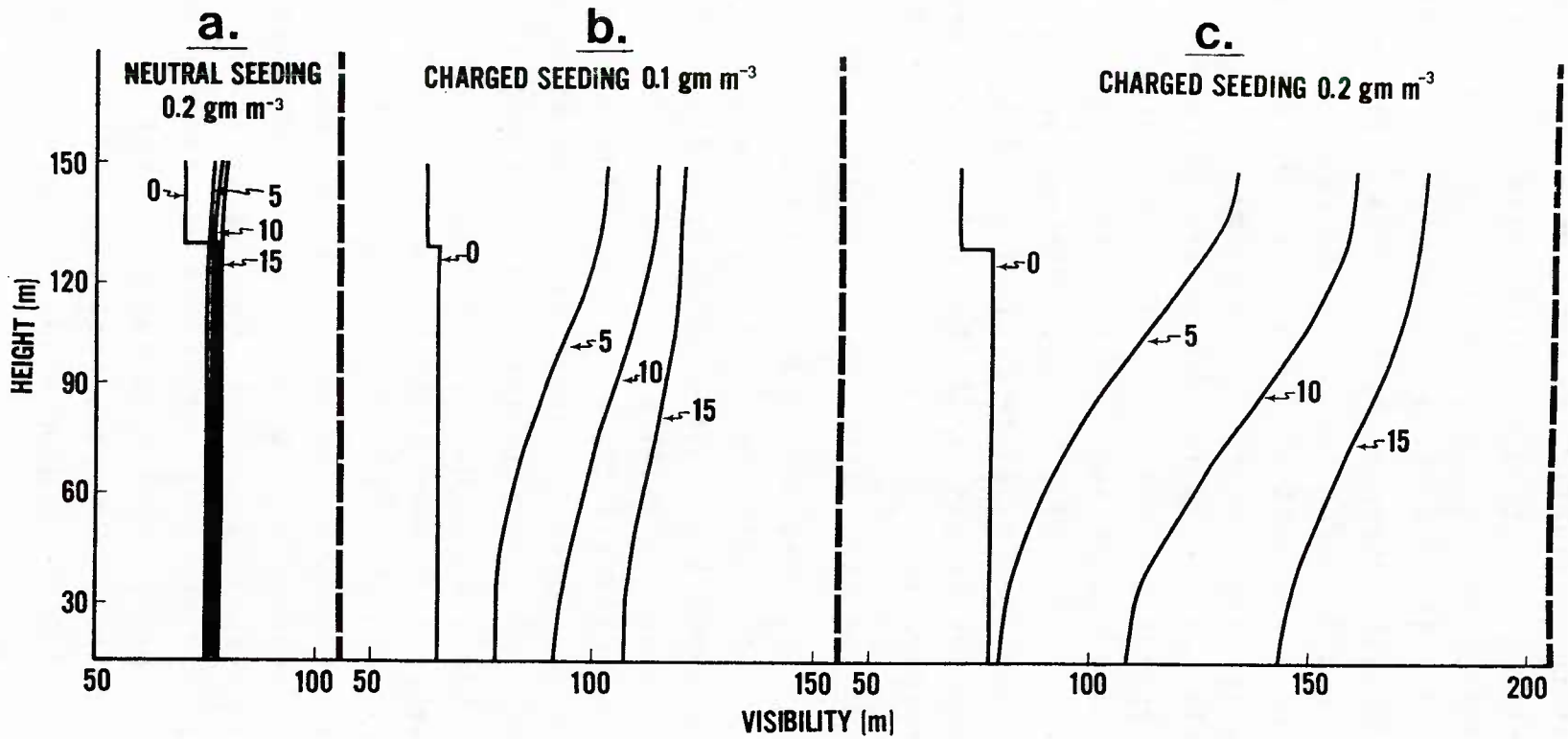

Figure 9. Visibility as a function of time (min) and height for three seeding variations in Fog B.

Examination of the visibility response shows a considerable decrease in effect -- noting that the scale of the abscissa has been changed. Defining a visibility improvement factor (VIF) as the visibility after 15 min divided by the initial visibility, the VIF decreases by more than a factor of two in going from Fog A to Fog B. Such a decrease is consistent with collection kernel ratios (noted earlier) using average radii for the two fog spectra (11 vs 3 μm). Figure 10, showing the time change of fog and treatment LWC's, indicates the smaller percentage (50% at 15 m) of fog water removal. A decrease in the downward speed of the treatment water maximum indicates further the reduction of treatment drop growth. As was also the case for Fog A, removal of fog droplets increases with increasing fog droplet size, but percentages have decreased considerably.

b. Experiment Set II - Variation of Seeding Drop Size

Experiment Set I established that the type of fog as well as the quantity of seeding material will affect the degree of visibility improvement. As is evident from Figure 3, the size of the seeding drops is equally, if not more, important than the size of the collected fog particles. The larger the collector drop the better. Unfortunately, an airborne spray system imposes limits on both the seeding rate and the quantity of available water. However, because Figure 3 is plotted "per drop" rather than normalized per unit of collector water volume, it fails to show that a halving in collector radius increases drop number density by a factor of eight (for the same LWC). Consequently, although the sweepout rate of a single smaller drop is less, the combined effect of several drops of that size can equal or exceed one larger drop. One could thus hypothesize that more and more smaller particles would be ever better. However, because the final terminal velocity of the collector drop should be large enough to

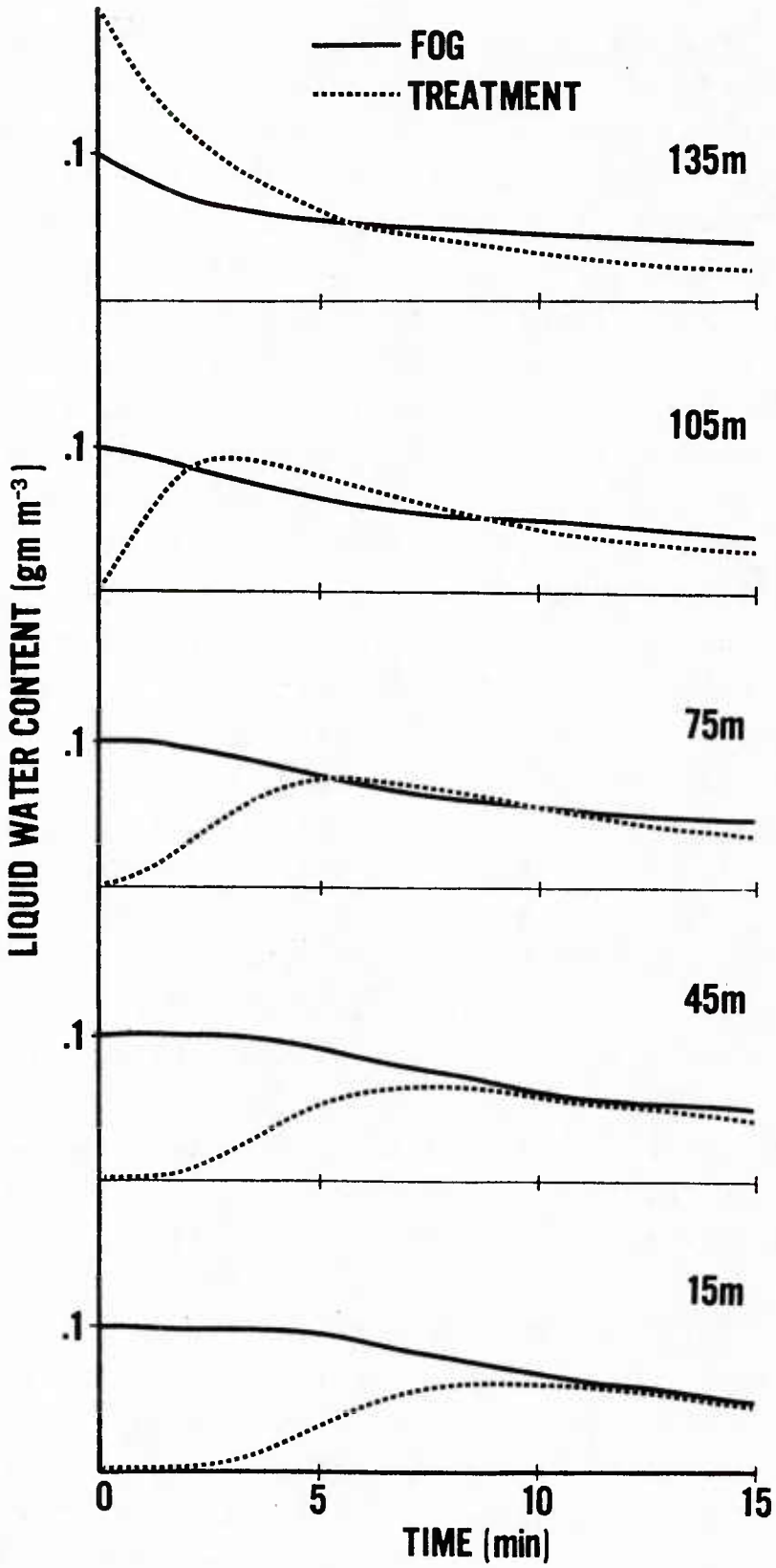

Figure 10. For alternate model levels, the change in fog and treatment LWC for experiment depicted in Figure 9c (Fog B with charged seeding of 0.2 gm m^{-3}).

allow it to fall from the fog, there must be a limit to which drop size can be reduced.

Several numerical experiments confirmed that a treatment LWC of 0.1 and 0.2 gm m^{-3} at larger mean sizes (than that of the spectrum in Figure 5) produced less visibility improvement. To determine if smaller sizes would be preferable, the cases described in Set I were repeated with a second seeding spectrum. All drop sizes shown in Figure 5 were arbitrarily divided by two (hereafter referred to as Seeding Spectrum II). LWC's were normalized to 0.1 and 0.2 gm m^{-3} as before, and a charge of 15% of the Rayleigh Limit was assigned to each category. The 22.2 μm mean radius of Seeding Spectrum I was thus changed to 11.1 μm in the new drop distribution.

Figures 11 and 12 show visibility changes for Fogs A and B, respectively, using Seeding Spectrum II. Neutral seedings are not known but, as before, produced negligible change. The charged seedings, however, produce more improvement in both fogs with both seeding concentrations than was previously produced with the larger sized seeding drops. Compared to Figures 8 and 10, Figures 13 and 14 show that more fog liquid water is removed in both fogs. Practically all of the fog LWC is removed in Fog A. Unfortunately, a considerable amount of the treatment, which contains the fog liquid water, is left behind. The improved visibilities created by Spectrum II suggests that, although approximately the same total amount of liquid water remains in the air (compared to Spectrum I), water has been transferred into larger, less visibility-restricting sizes. A similar change occurs in Fog B, but with even more total liquid remaining (comparing Figure 14 to Figure 10). Obviously, a relatively small concentration of seeding liquid can result in the collection of most of the fog drops. However, unless the growth of the seeding particles results in final sizes large enough to fall from the fog, the seeding material itself will remain to limit

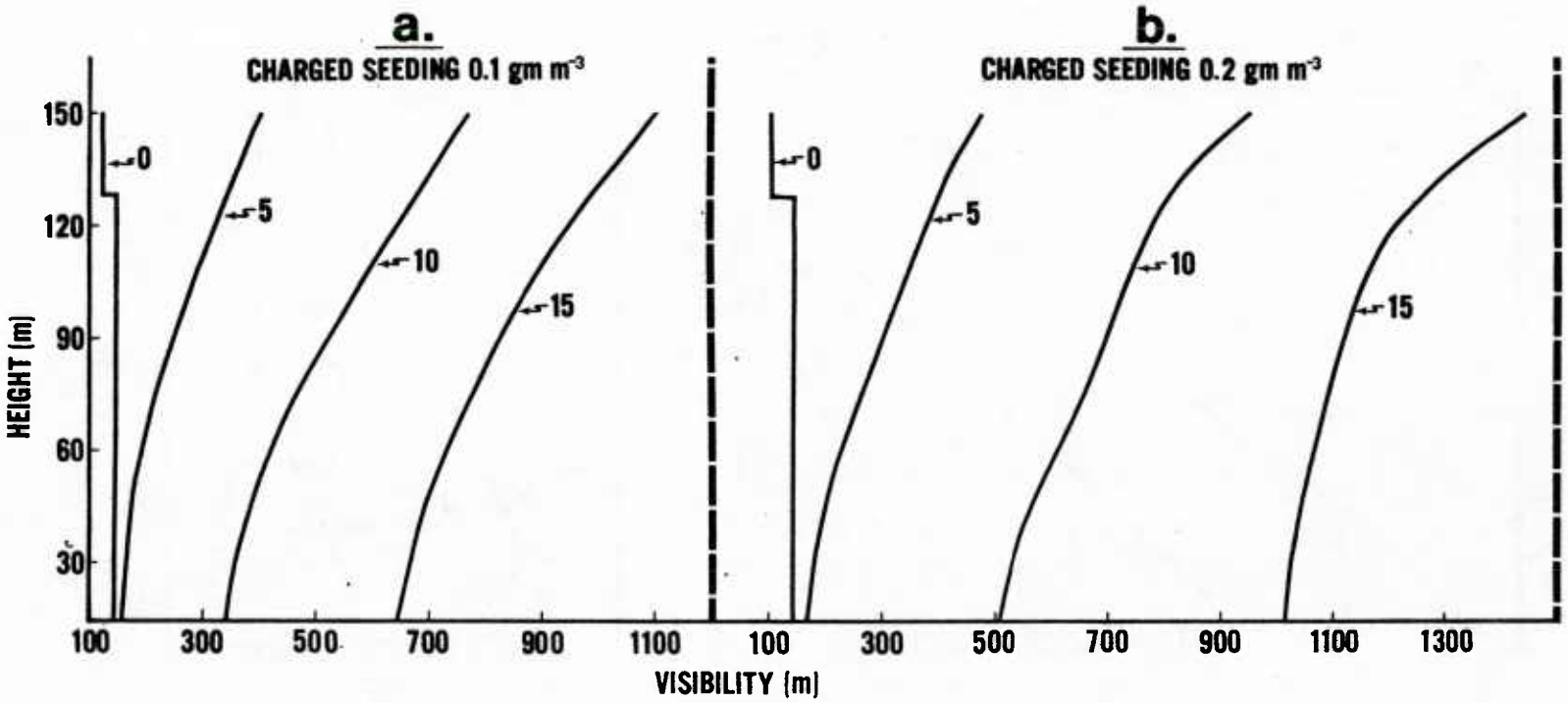

Figure 11. Visibility as a function of time (min) and height using Seeding Spectrum II in Fog A.

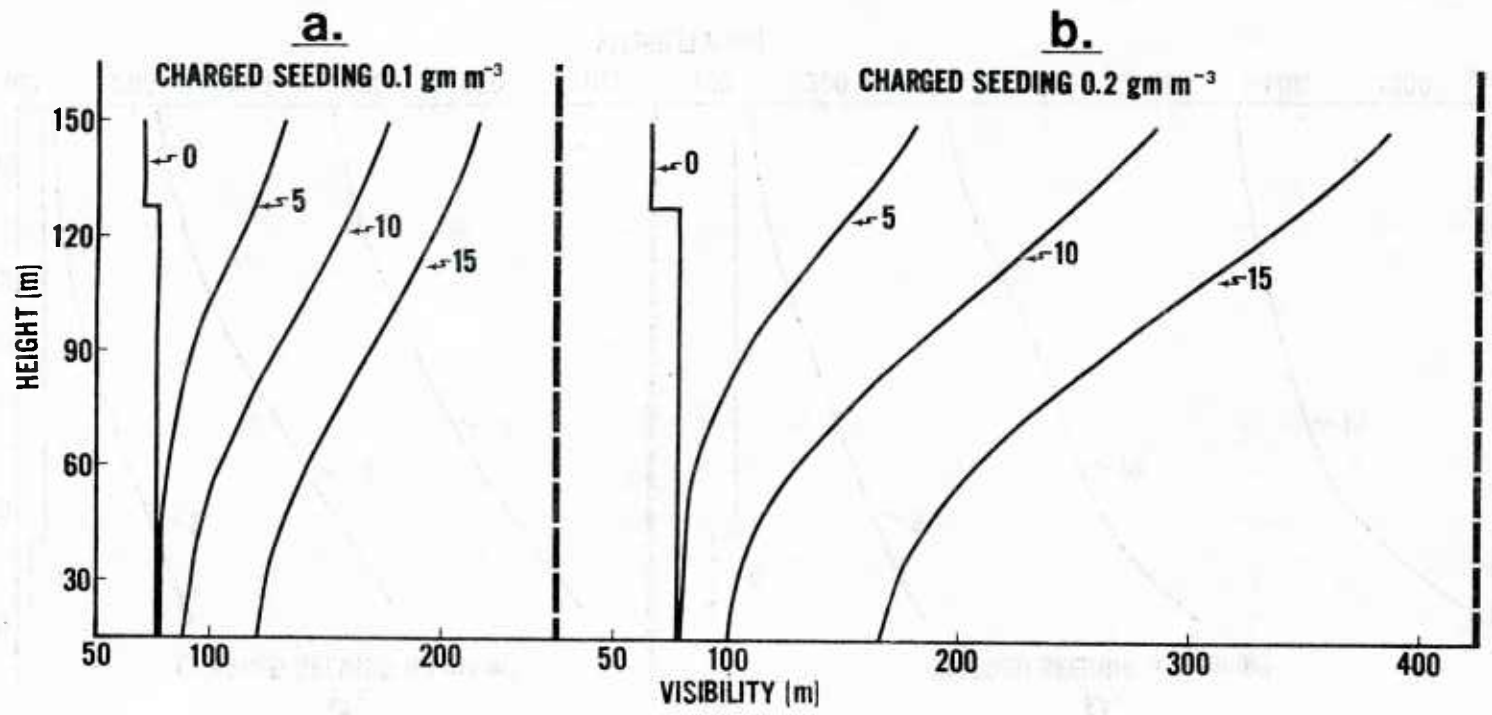

Figure 12. Visibility as a function of time (min) and height using Seeding Spectrum II in Fog B.

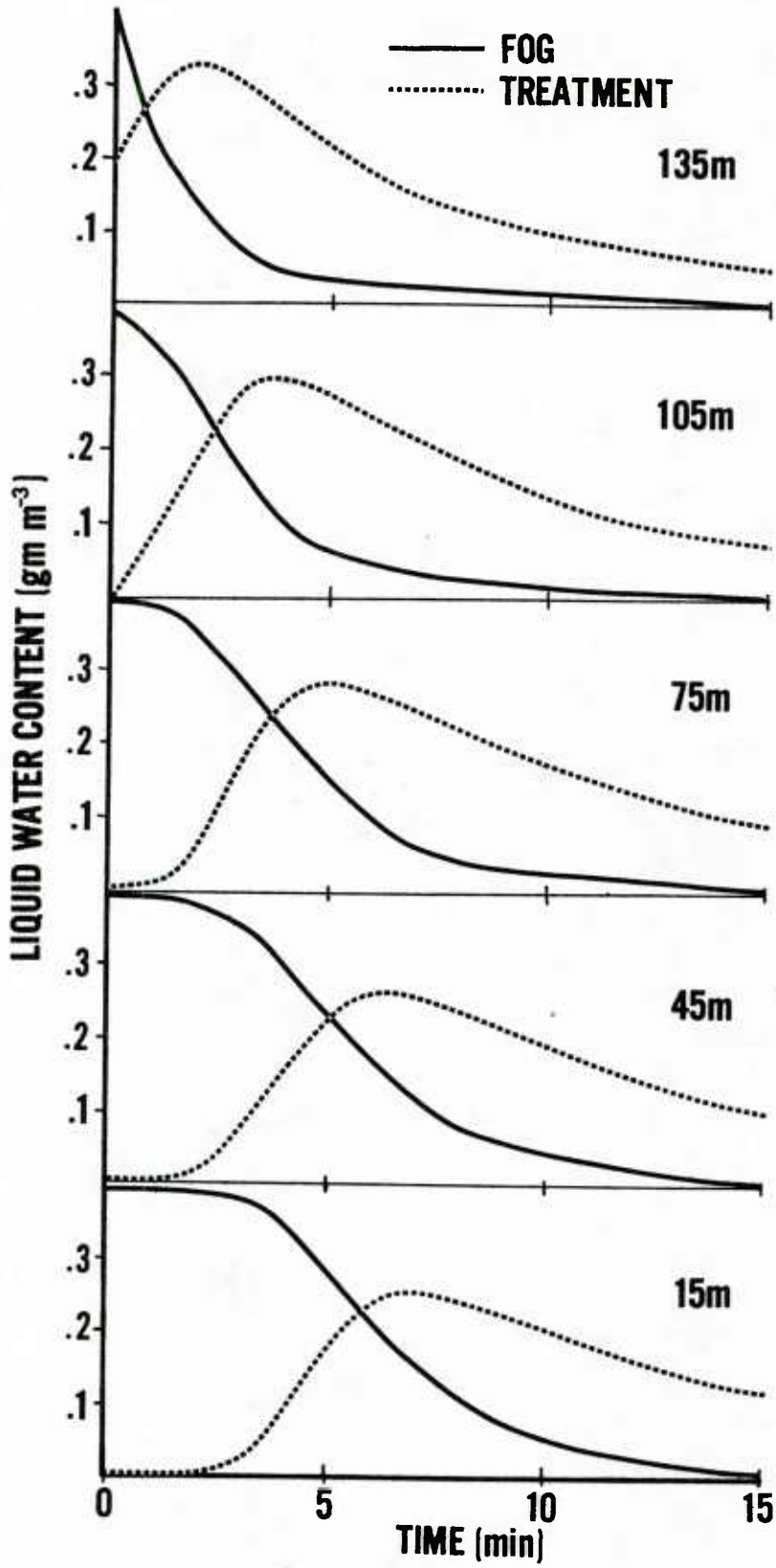

Figure 13. For alternate model levels, the change in fog and treatment LWC for experiment depicted in Figure 11b (Fog A with charged Seeding Spectrum II seeding of 0.2 gm m^{-3}).

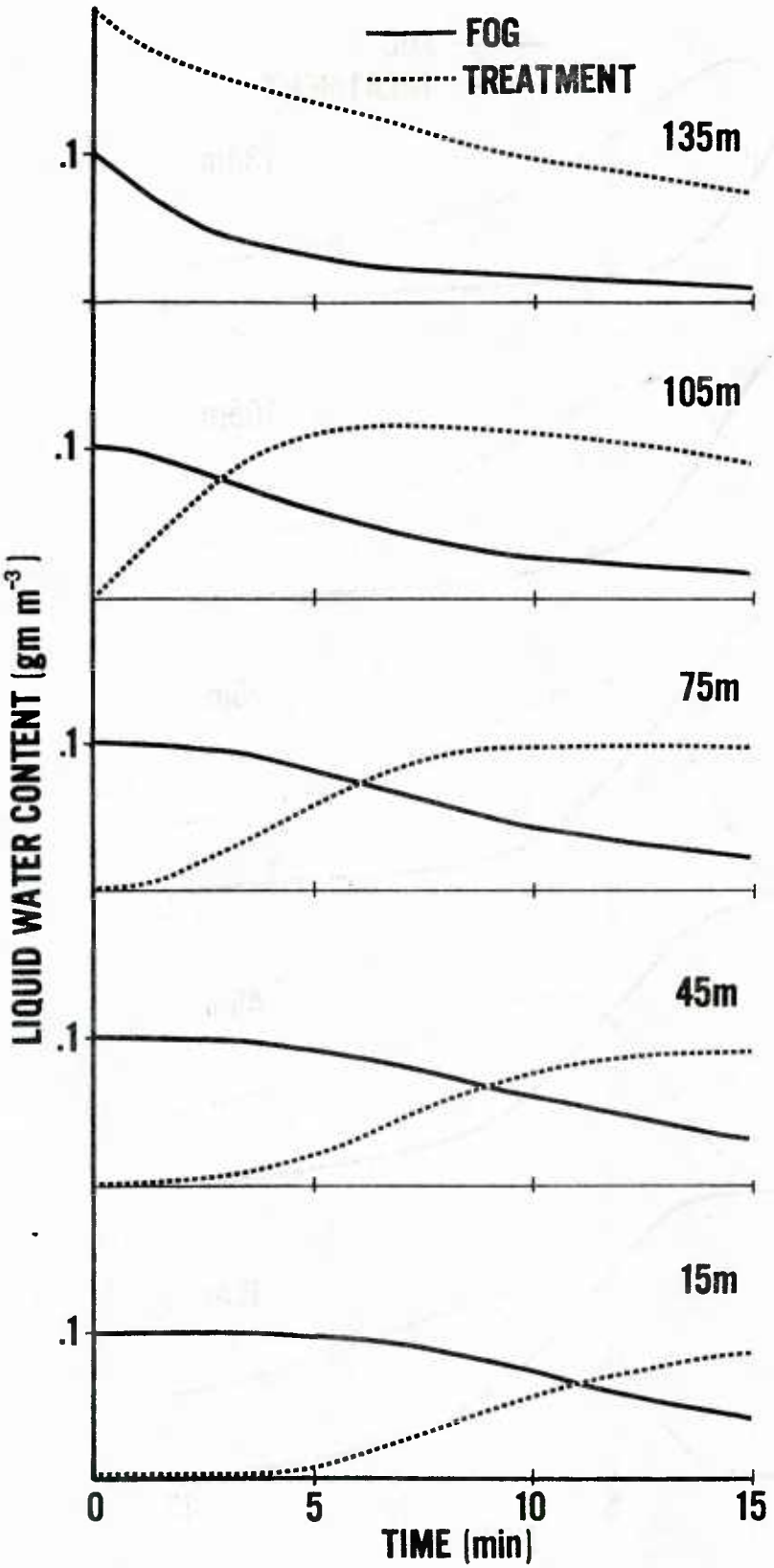

Figure 14. For alternate model levels, the change in fog and treatment LWC for experiment depicted in Figure 12b (Fog B with charged Seeding Spectrum II seeding of 0.2 gm m^{-3}).

visibility somewhat. Unlike the earlier study of an applied electric field in which visibility improvement resulted primarily from removal of fog water, seeding with charged drops produces visibility change both from this removal and from a movement of water from the fog to the treatment spectrum. Because most seeding drops are significantly larger in size than the fog droplets, movement of water from small visibility-restricting sizes to larger less-restricting radii is significant.

Subsequent reductions in treatment drop size caused maximum visibilities, in both fogs, either to decrease or remain about the same. In general, although more and more fog water was collected, more total water remained behind. And, because this remaining water is associated with average sizes smaller than those associated with larger initial treatment drops, visibility decreases. It would thus appear that, with the concentrations that can be produced by current research aircraft, a treatment distribution averaging between 10 and 15 μm in radius is ideal.

c. Experiment Set III - Variation of Treatment Concentration

It was earlier evident that a treatment concentration of 0.2 gm m^{-3} produced better results than half that amount. With the idea that more is always better, Fogs A and B were seeded with ever larger concentrations. One would expect, however, that a point would be reached beyond which increased seeding would prove detrimental. Such was shown to be true for hygroscopic seeding of warm fogs (see, e.g., Tag *et al.*, 1970 or Silverman and Kunkel, 1970). Although the basic mechanism (condensation) for that technique is different, the effect caused by over-seeding is the same -- too many particles competing for the available water, growing too little, and remaining in the fog.

Figure 15 summarizes final visibility (after 15 min) as a function of initial treatment concentration. Both Fogs A and B and Seeding Spectra I and II are considered. Visibility at the lower of the two seeding levels (135 m, level 9) is plotted. Obviously, an optimum concentration for one fog and seeding spectrum is not the same as for others. In general, as the mean radius of the seeding spectrum decreases, smaller concentrations become optimum. It must be remembered, however, that the operational situation described earlier could only produce average concentrations on the order of 0.1 gm m^{-3}. As a result, unless a particular area were repeatedly treated with multiple seeding passes, the threat of over-seeding is not a concern. Even small pockets of initially large concentrations left in the seeding wake should not remain for very long. As is evident from Figure 15, for the seeding spectrum currently in use in the field (Spectrum I), seeding rates could be increased up to eight times with ever better results.

d. Experiment Set IV - Variation of Seeding Drop Charge

A comparison of the collection kernels in Figures 3b and c, for 15 and 30% of the Rayleigh Limit respectively, shows the effect of increased charge. Equation (2) indicates that a doubling of charge results in a 1.74 increase in collision efficiency, and thus the sweepout rate. Several experiments were conducted to determine how this increase is translated into visibility improvement.

An initial charge of 30% of the Rayleigh Limit was tried with both seeding spectra in both fogs. It was found that a doubling of charge results, generally, in a doubling of visibility improvement. No significant trends were discovered for either fog or seeding spectrum. The charge increase

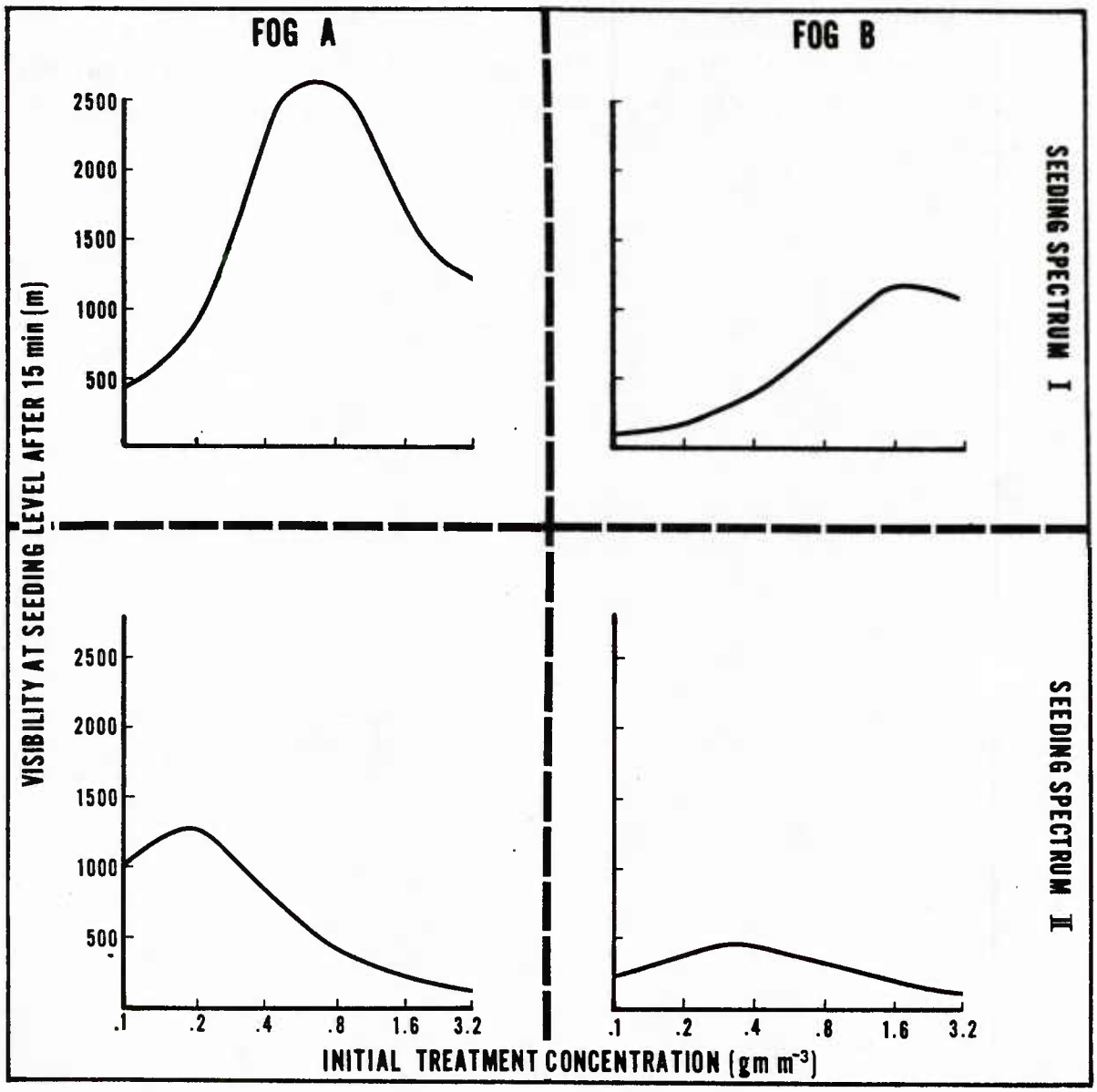

Figure 15. Final visibility as a function of initial treatment concentration for both seeding spectra in both fogs.

gave a slightly larger percentage of improvement in the lower fog levels. Also, those situations which had resulted in large improvements for the 15% seedings gave smaller percentage increases than those situations which had responded poorly. Technical considerations in the field will surely dictate limits to the eventual seeding drop charge, but theory suggests that charge be maximized as fully as possible.

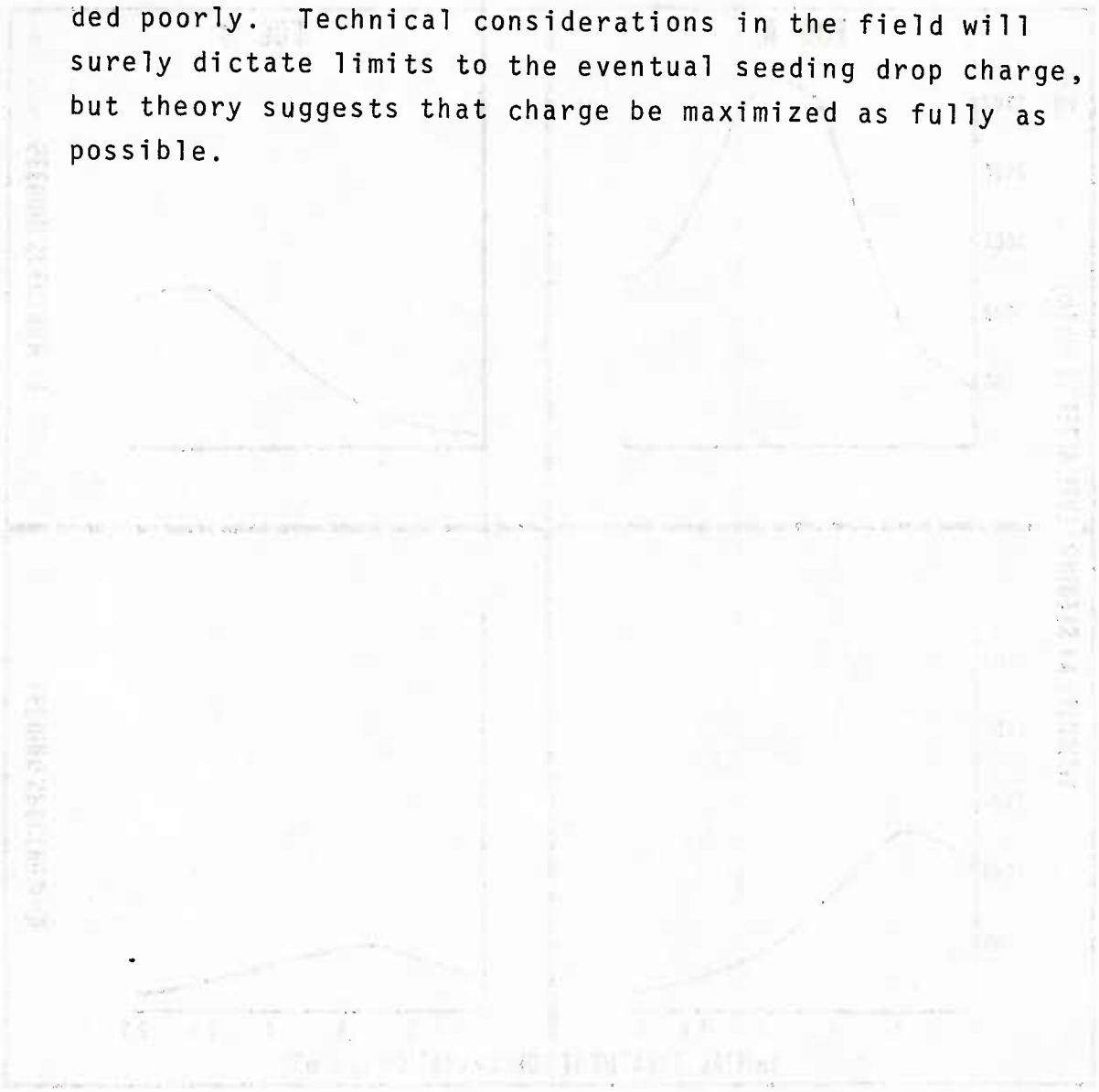

7. AN EVALUATION

From this study alone, a complete evaluation of the feasibility of using charged water drops to clear fog is impossible. The one-dimensionality of the model has precluded processes which would tend to limit clearing potential. In addition, there are currently no field test data with which to compare the results. A comparison to the earlier-mentioned study by Carroz et al. is not feasible because of the different nature of that study. In addition to using monodisperse spectra, hygroscopic growth was included in the growth of drops charged completely to the Rayleigh Limit.

One comparison which is of significance relates to earlier numerical studies of hygroscopic seeding of warm fogs. Of these studies, one was made using basically the same model as that used in this study (see, e.g., Tag et al. (1970) or Tag (1971)). Condensation, rather than collection growth, was the important mechanism in the hygroscopic simulations. To allow an accurate comparison between hygroscopic and charged drop seedings, several hygroscopic seeding experiments were repeated using treatment concentrations and spectra duplicating those used in this study. As in the earlier hygroscopic seeding studies and that described by Carroz et al., a mixture of urea, ammonium nitrate, and water is the hygroscopic solution being simulated.

Figures 16 and 17 represent hygroscopic seedings of Fogs A and B using a concentration of 0.1 gm m^{-3} with Seeding Spectrum I. They can be compared directly to Figures 7b and 9b, respectively. Note that the abscissa is now logarithmically, rather than linearly, scaled. Obviously, the model predicts that hygroscopic seedings will result in much more visiblity improvement. VIF's are one to two orders of magnitude greater than those from the charged seedings.

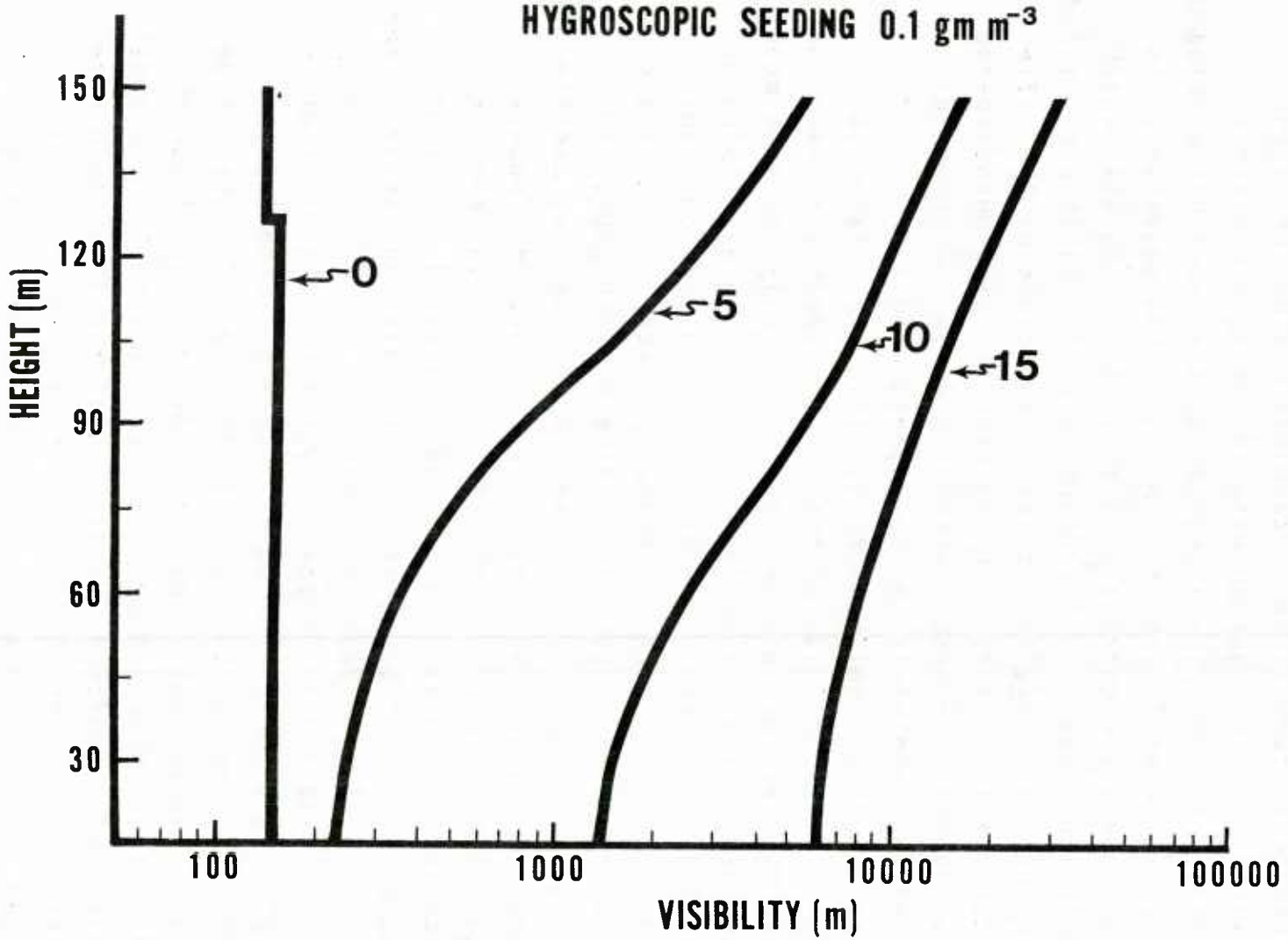

Figure 16. Visibility as a function of time (min) and height using a hygroscopic Seeding Spectrum I in Fog A.

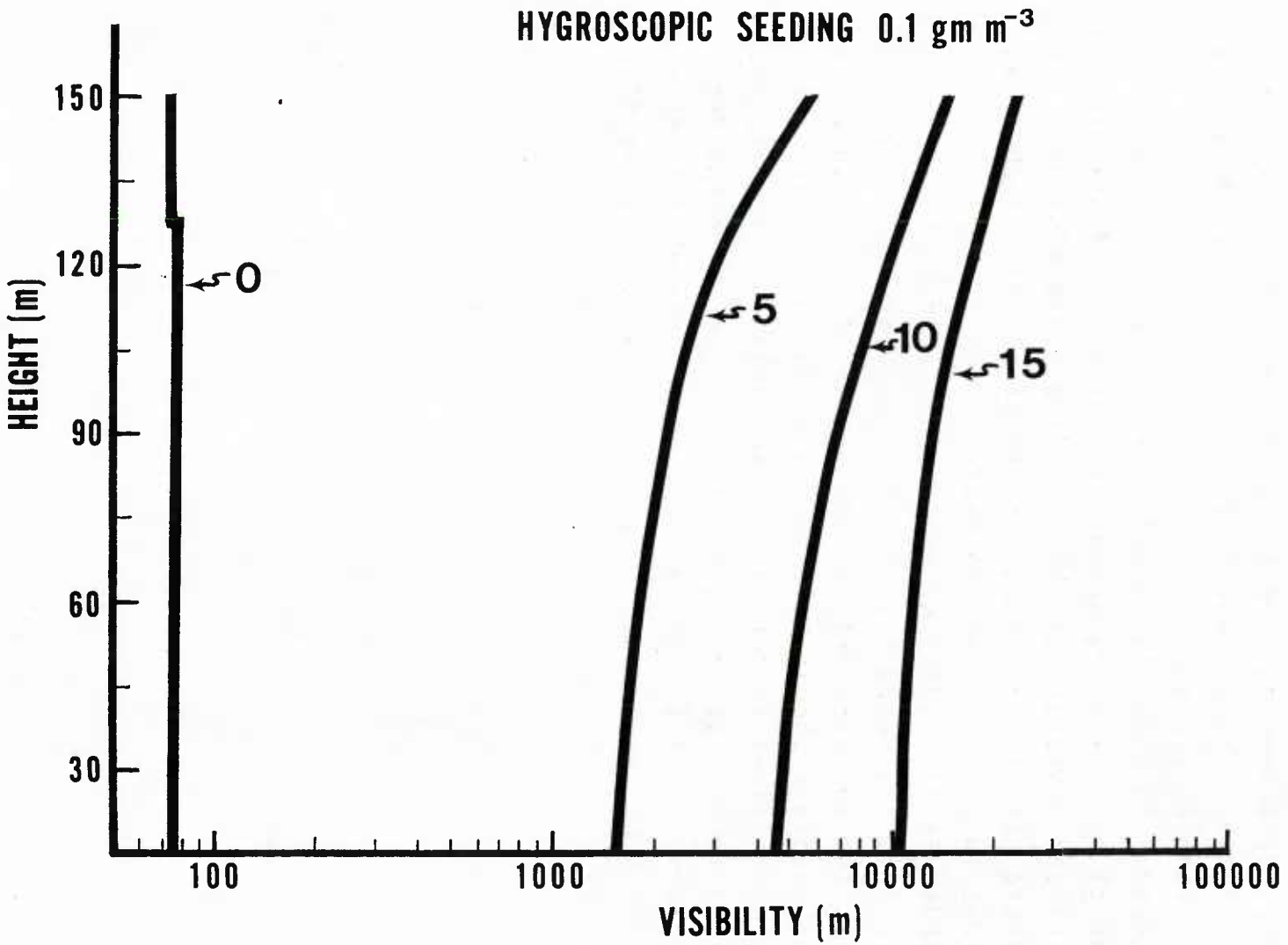

Figure 17. Visibility as a function of time (min) and height using a hygroscopic Seeding Spectrum I in Fog B.

In contrast to the potential suggested by numerical modeling (see also Silverman and Kunkel (1970)), field studies of hygroscopic seeding have produced inconsistent results. Under relatively stable maritime conditions, St. Amand et al. (1971) produced repeatable clearings in seven out of seven experiments; in later tests at the same location, however, Hindman et al. (1973) reported that three out of six experiments raised visibilities above landing field minimums. In a separate set of experiments, Smith et al. (1970) observed clearings in three out of ten tests.

Thus, field studies of hygroscopic seeding have not borne out the potential suggested by numerical modeling. Consequently, the above numerical comparisons of hygroscopic and charged seedings should hold some significance. They suggest that the treatment concentrations and charges that have been simulated in this paper are not adequate for clearing fog. Furthermore, it is concluded that, unless concentrations and charges can be very greatly increased, charged drop seeding may not be a viable fog dissipation technique.

8. CONCLUSIONS

The following specific conclusions were reached from the modeling experiments:

(1) Visibility improvement is closely linked to the size of the fog droplets. For the same treatment spectrum, visibility improvement decreases with the average fog droplet size.

(2) For the same amount of seeding water, a treatment spectrum with an average size between 10 and 15 μm is ideal. A distribution having too much water concentrated in radii less than 10 μm results in drops which, after growth, have fall velocities that are too small. A distribution with too many large drops -- although each drop is quite efficient as a collector -- does not possess the number density required to optimally improve visibility.

(3) For an applied electric field, it was shown that visibility improvement results primarily from droplet fallout caused by spectral widening. With charged drop seeding, improvement results both from a removal of fog water (to the ground) and from a transfer of water from the fog spectrum to the larger treatment drops.

(4) Visibility improvement increases with seeding rate. For a given seeding spectrum, a theoretical point of over-seeding is possible but unlikely with concentrations generated by current airborne systems capable of dispensing charged water drops.

(5) Visibility improvement increases with seeding drop charge. This charge should be maximized as fully as possible.

The following conclusions were reached by comparing results of this study to results of simulations of hygroscopic seeding:

(1) The charges and treatment concentrations that have been simulated in this paper would not be adequate for clearing fog.

(2) Unless charges and seeding concentrations can be very greatly increased, charged drop seeding is probably not a viable fog dissipation technique.

It is hoped that results from future field experiments will allow comparisons which test these latter two conclusions.

REFERENCES

Anonymous, 1923: Sand-blasting the clouds for man-made weather. Sci. Amer., 128, 224.

Berry, E.X., 1967: Cloud droplet growth by collection. J. Atmos. Sci., 24, 688-701.

Carroz, J.W., P. St. Amand, and D.R. Cruise, 1972: The use of highly charged hygroscopic drops for fog dispersal. J. Wea. Mod., 4, No. 1, 54-69.

Carroz, J.W. and P.N. Keller, 1976: Electrostatic induction parameters to attain maximum spray charge. Naval Weapons Center Tech. Pub. 5796, 30 pp.

Cochet, R., 1952: L'evolution d'une gouttelette d'eau chargee dans un nuage ou un brouillard a temperature positive (The growth of a charged water drop in a cloud at temperatures above freezing). Annales de Geophysique, 8, 33-54.

Davis, M.H., 1964: Two charged spherical conductors in a uniform electric field: forces and field strength. Quart. J. Mech. Appl. Math., 17, 499-511.

Davis, M.H. and J.D. Sartor, 1967: Theoretical collision efficiencies for small cloud droplets in Stoke's flow. Nature, 215, 1371-1372.

Hendricks, C.D., 1962: Charged droplet experiments. J. Colloid Sci., 17, 249-259.

Hindman II, E., R.S. Clark, and P. St. Amand, 1973: Project Foggy Cloud IV - Phase I. Evaluation of warm fog dissipation techniques. Naval Weapons Center, China Lake, Ca., Tech. Pub. 5413, 52 pp.

Johnson, D.B., 1972: Visibility calculations for microphysical computer models. Environmental Prediction Research Facility, Monterey, CA, Tech. Note No. 5-72, 23 pp. (DDC or NTIS AD 776-208).

Moore, A.D., 1973: Electrostatics and its applications. John Wiley and Sons, New York, 481 pp.

Paluch, I.R., 1970: Theoretical collision efficiencies of charged cloud droplets. J.G.R., 75, 1633-1640.

Pauthenier, M., 1950: Electrical coalescence of fogs and clouds. Royal Meteorological Society, Centenary Proceedings, 60-61.

Rayleigh, L., 1879: The influence of electricity on colliding water drops. Proc. Roy. Soc., 28, 406-409.

Rayleigh, L., 1882: On the equilibrium of liquid conducting masses charged with electricity. Phil. Mag., 14, 184-186.

Reinking, R.F., 1975: Project Foggy Cloud VII -- Warm Fog dispersal and prevention (prelimina;ry summary). Naval Weapons Center Tech. Mem. 2527, 30 pp.

Schweizer, J.W. and D.N. Hanson, 1971: Stability limit of charged drops. J. Coll. and Interface Sci., 35, 417-423.

Shafrir, V. and M. Neiburger, 1963: Collision efficiencies of two spheres falling in a viscous medium. J. Geophys. Res., 68, 4141-4148.

Silverman, B.A. and B.A. Kunkel, 1970: A numerical model of warm fog dissipation by hygroscopic particle seeding. J. Appl. Meteor., 9, 627-633.

Smith, T.B. and P.B. MacCready, 1963: Aircraft wakes and diffusion enhancement. MRI 63 FR-71, 14 pp.

Smith, T.B., C.W. Chien, and A.I. Weinstein, 1970: Warm fog modification. Final Report AFCRL-70-0105, Meteorology Research, Inc., Altadena, CA.

St. Amand, P., R.S. Clark, T.L. Wright, W.G. Finnegan, and E.A. Blomerth, Jr., 1971: Warm fog modification. Preprints Intern. Conf. Weather Modification, Canberra, Australia, Amer. Meteor. Soc., 259-264.

Tag., P.M., D.B. Johnson and E.E. Hindman II, 1970: Engineering fog-modification experiments by computer modeling. Preprints, Second National Conference on Weather Modification, Amer. Meteor. Soc., 97-102.

Tag, P.M., 1971: Results generated from a one-dimensional warm fog model which simulates hygroscopic seeding. Navy Weather Research Facility, Norfolk, VA, Tech. Paper No. 11-71, 63 pp. (DDC or NTIS AD769-226).

Tag, P.M., 1976: A numerical simulation of warm fog dissipation by electrically enhanced coalescence: Part I. An applied electric field. J. Appl. Meteor., 15, 282-291.

Tate, R.W. and E.O. Olson, 1962: Spray droplet size of pressure-atomizing burner nozzles. ASHRAE Journal, March 1962, 39-42.

Weinstein, A.I. and B.A. Silverman, 1973: A numerical analysis of some practical aspects of airborne urea seeding for warm fog dispersal at airports, J. Appl. Meteor., 12, 771-780.

Wobus, H.B., F.W. Murray and L.R. Koenig, 1971: Calculation of the terminal velocity of water drops. J. Appl. Meteor., 10, 751-754.